












ARTICLE

<https://doi.org/10.1038/s41467-019-11255-0>

OPEN

A plasmid-encoded peptide from *Staphylococcus aureus* induces anti-myeloperoxidase nephritogenic autoimmunity

Joshua D. Ooi¹, Jhih-Hang Jiang ², Peter J. Eggenhuizen ¹, Ling L. Chua ^{1,14}, Mirjan van Timmeren³, Khai L. Loh ⁴, Kim M. O'Sullivan¹, Poh Y. Gan¹, Yong Zhong¹, Kirill Tsyganov ⁵, Lani R. Shochet^{1,6}, Jessica Ryan^{1,6}, Coen A. Stegeman⁷, Lars Fugger ⁸, Hugh H. Reid ^{4,9}, Jamie Rossjohn ^{4,9,10}, Peter Heeringa ³, Stephen R. Holdsworth^{1,6}, Anton Y. Peleg ^{2,11} & A. Richard Kitching ^{1,6,12,13}

Autoreactivity to myeloperoxidase (MPO) causes anti-neutrophil cytoplasmic antibody (ANCA)-associated vasculitis (AAV), with rapidly progressive glomerulonephritis. Here, we show that a *Staphylococcus aureus* peptide, homologous to an immunodominant MPO T-cell epitope (MPO₄₀₉₋₄₂₈), can induce anti-MPO autoimmunity. The peptide (6PGD₃₉₁₋₄₁₀) is part of a plasmid-encoded 6-phosphogluconate dehydrogenase found in some *S. aureus* strains. It induces anti-MPO T-cell autoimmunity and MPO-ANCA in mice, whereas related sequences do not. Mice immunized with 6PGD₃₉₁₋₄₁₀, or with *S. aureus* containing a plasmid expressing 6PGD₃₉₁₋₄₁₀, develop glomerulonephritis when MPO is deposited in glomeruli. The peptide induces anti-MPO autoreactivity in the context of three MHC class II allomorphs. Furthermore, we show that 6PGD₃₉₁₋₄₁₀ is immunogenic in humans, as healthy human and AAV patient sera contain anti-6PGD and anti-6PGD₃₉₁₋₄₁₀ antibodies. Therefore, our results support the idea that bacterial plasmids might have a function in autoimmune disease.

¹ Centre for Inflammatory Diseases, Monash University Department of Medicine, Monash Medical Centre, Clayton, VIC 3168, Australia. ² Infection and Immunity Program, Monash Biomedicine Discovery Institute and Department of Microbiology, Monash University, Clayton, VIC 3800, Australia.

³ Department of Pathology and Medical Biology, University of Groningen, University Medical Center Groningen, Groningen 9700 RB, The Netherlands.

⁴ Infection and Immunity Program and Department of Biochemistry and Molecular Biology, Biomedicine Discovery Institute, Monash University, Clayton, VIC 3800, Australia. ⁵ Monash Bioinformatics Platform, Monash University, Clayton, VIC 3800, Australia. ⁶ Department of Nephrology, Monash Health, Clayton, VIC 3168, Australia. ⁷ Department of Internal Medicine, Division of Nephrology, University of Groningen, University Medical Center Groningen, Groningen 9700 RB, The Netherlands. ⁸ Oxford Centre for Neuroinflammation, Nuffield Department of Clinical Neurosciences, and MRC Human Immunology Unit, Weatherall Institute of Molecular Medicine, John Radcliffe Hospital, University of Oxford, Oxford OX3 9DS, UK. ⁹ Australian Research Council Centre of Excellence in Advanced Molecular Imaging, Monash University, Clayton, VIC 3800, Australia. ¹⁰ Institute of Infection and Immunity, School of Medicine, Cardiff University, Cardiff CF14-4XN, UK. ¹¹ Department of Infectious Diseases, Alfred Hospital and Central Clinical School, Monash University, Melbourne, VIC 3004, Australia. ¹² NHMRC Centre for Personalised Immunology, Monash University, Clayton, VIC 3168, Australia. ¹³ Department of Pediatric Nephrology, Monash Health, Clayton, VIC 3168, Australia. ¹⁴ Present address: Department of Paediatrics, Faculty of Medicine, University of Malaya, Kuala Lumpur 50603, Malaysia. Correspondence and requests for materials should be addressed to A.R.K. (email: richard.kitching@monash.edu)

Loss of tolerance to the neutrophil enzyme myeloperoxidase (MPO) leads to anti-neutrophil cytoplasmic antibody (ANCA)-associated vasculitis (MPO-AAV), an autoimmune disease that can affect multiple tissues but which often involves the kidney. In MPO-AAV, patients frequently develop rapidly progressive glomerulonephritis and are at risk of end-stage kidney failure¹. The other major autoantigen known to be clinically relevant in AAV is the neutrophil serine protease, proteinase-3 (PR3). MPO-AAV and PR3-AAV, while having some differences, share similar pathogenic features. In MPO-AAV, tissue injury is induced not by autoantibodies binding to target tissues such as the kidney, but by anti-MPO autoantibodies (MPO-ANCA) that bind to and activate neutrophils causing glomerular neutrophil recruitment, degranulation, and NETosis^{2–4}. These activated neutrophils are not only themselves responsible for significant tissue injury and damage, they also deposit MPO in and around glomerular capillaries^{2,4–6}. Thus, MPO accumulating in glomeruli may function as an antigenic target for MPO-specific effector CD4⁺ and CD8⁺ T cells that induce a further wave of cell-mediated injury^{3,6–9}.

Although it is unclear how tolerance to neutrophil cytoplasmic antigens MPO and proteinase-3 (PR3) is lost and how disease is triggered¹⁰, like many autoimmune diseases¹¹, both genetic and environmental factors are probably important^{12,13}. In particular, infection has been implicated both in clinical studies, and in in vitro and in vivo experimental work^{5,14–17}. Nasal carriage of *Staphylococcus aureus* is associated with an increase in relapse of disease in granulomatosis with polyangiitis, characterized by loss of tolerance to PR3 (PR3-AAV)¹⁴. Less is known about *S. aureus* colonization of people with MPO-AAV. While chronic nasal carriage is uncommon in those with microscopic polyangiitis and renal limited vasculitis, usually associated with MPO-ANCA¹⁸, nasal colonization does occur¹⁹ and case reports implicate *S. aureus* in the development of this condition^{20–22}. There are several mechanisms by which infections might influence AAV; superantigens have been hypothesized to have a function²³, and pathogen-associated molecular patterns stimulate antigen presentation, B cells, and prime neutrophils²⁴. The release of autoantigens (including PR3 and MPO) by neutrophils at sites of infection might also affect the maintenance of tolerance. A further potential consequence of the uptake of neutrophil-derived autoantigens by antigen-presenting cells at sites of inflammation with innate immune system activation could be the development of molecular mimicry. As molecular mimicry can lead to T-cell receptor (TCR) cross-reactivity^{25–28}, a microbial mimotope presented as a peptide by MHC Class II (MHCII) might activate TCRs that also recognize PR3 or MPO-derived epitopes presented by MHCII.

Some evidence supports the involvement of molecular mimicry in the loss of tolerance to neutrophil antigens in AAV. The complementary PR3 autoantigenic sequence, implicated in loss of tolerance to PR3, shares homology with bacterial peptides, including some from *S. aureus*²⁹. Another target neutrophil antigen, lysosomal antigen membrane protein-2 (LAMP-2), shares sequence homology with the bacterial adhesin FimH, with FimH immunization of rats inducing anti-LAMP-2 autoantibodies and glomerulonephritis³⁰. However, it is not known whether molecular mimicry has any function in loss of tolerance to MPO and the resultant development of MPO-AAV.

Here, we demonstrate that molecular mimicry mechanistically contributes to the loss of tolerance to MPO in AAV. We evaluate whether microbial-derived peptides, including those from *S. aureus*, with sequence homology to the immunodominant MPO CD4⁺ T-cell epitope can induce the expansion of naive CD4⁺ T cells that recognize MPO, with the subsequent development of cross-reactive anti-MPO autoimmunity leading to

glomerulonephritis and AAV. We identify a *S. aureus* peptide, 6-phosphogluconate dehydrogenase (6PGD)_{391–410} derived from a plasmid-encoded protein that induces cellular and humoral anti-MPO autoimmunity and experimental anti-MPO glomerulonephritis. Thus, molecular mimicry mediated by a bacterial plasmid capable of horizontal transmission represents a potential mechanism of loss of tolerance in autoimmune disease.

Results

Highly homologous peptides do not induce autoreactivity. To determine if autoreactivity to the immunodominant MPO CD4⁺ T-cell epitope, mouse MPO_{409–428}⁶, could be induced by microbial peptides, we performed a protein BLAST (blastp) search using the core 11-mer sequence of the equivalent human MPO peptide, ₄₄₁RLYQEARKIVG₄₅₁ (mouse MPO peptide sequence and numbering: ₄₁₅KLYQEARKIVG₄₂₅). Sequences from the Animalia kingdom (taxid:33208) and microbes not known to colonize humans were excluded. Based on the search results, we selected the four most homologous sequences (Supplementary Table 1) and because we have demonstrated previously that a 20-mer peptide induces stronger immunoreactivity to MPO⁶ (concordant with MHCII molecules having an open ended binding groove³¹), we synthesized 20-mers based on the four identified sequences. For example, for the *Aspergillus fumigatus* HEAT repeat protein_{831–841} (₈₃₁RWYQEARKIIF₈₄₁) the synthesized 20-mer was ₈₂₅ISALPQRWYQEARKIIF₈₄₄. To determine whether these sequences could induce anti-MPO autoimmunity we immunized C57BL/6 mice with individual 20-mers and measured T-cell reactivity to either the immunizing peptide, MPO_{409–428}, or recombinant mouse (rm)MPO using interferon- γ (IFN- γ) and interleukin (IL)-17A ELISPOTs and [³H]-T proliferation assays. While some homologous sequences induced reactivity to themselves, none induced reactivity to MPO_{409–428} or whole rmMPO (Fig. 1a–f), demonstrating that high sequence homology per se does not result in immunological cross-reactivity to MPO.

A *S. aureus*-derived peptide induces anti-MPO autoimmunity.

As *S. aureus* infections can precede the development of MPO-AAV^{20–22}, they are related to an overlapping form of vasculitis (PR3-AAV)^{14,29} and nasal colonization of *S. aureus* has been found in people with MPO-AAV¹⁹ we identified a *S. aureus*-derived peptide with sequence homology to human MPO_{441–451} by protein BLAST. The highest scoring *S. aureus*-derived peptide containing the previously defined critical MPO_{441–451} T-cell epitope residues (Tyr443, Arg447, Ile449 and Val450: ₄₄₁RLYQEARKIVG₄₅₁)⁶ was selected (BLAST MAX score of 18.0 out of 38.4 compared to human MPO_{441–451}). The identified peptide, 6PGD_{397–408} (₃₉₇TDYQEALRDVVA₄₀₈) was from 6-phosphogluconate dehydrogenase (6PGD), an enzyme of the pentose phosphate pathway, and was first described within the plasmid pSJH101 from the clinically relevant *S. aureus* strain JH1³². To determine whether this 6PGD_{397–408} sequence induced autoimmunity to MPO, we immunized C57BL/6 mice with 6PGD_{391–410} (₃₉₁YFKNIVTDYQEALRDVVATG₄₁₀). Mice developed reactivity to 6PGD_{391–410}, as well as autoreactivity to both the immunodominant MPO CD4⁺ T-cell epitope, MPO_{409–428}, and to rmMPO (Fig. 2a). MPO_{409–428}-immunized mice served as a positive control. To determine if exposure to 6PGD_{391–410} induces in vivo expansion of MPO-specific T cells, we immunized mice with 6PGD_{391–410} then enumerated the number of MPO-specific T cells using an I-A^b tetramer presenting the core mouse MPO T-cell epitope (₄₁₅KLYQEARKIVG₄₂₅). We compared the total numbers of MPO-specific T cells from naive mice, OVA_{323–339} immunized mice and

Immunizing peptide antigens:

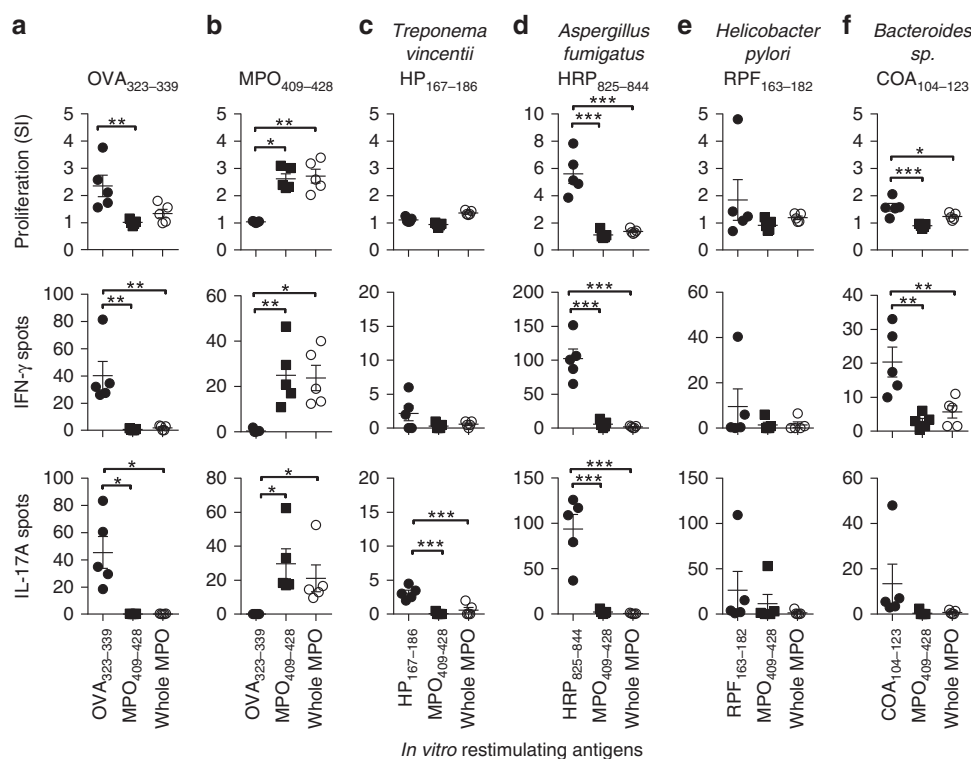


Fig. 1 Microbe-derived peptides with closest sequence homology to MPO₄₀₉₋₄₂₈ do not induce cross-reactivity to MPO. C57BL/6 mice ($n = 5$ each group) were immunized with peptides, either **a** OVA₃₂₃₋₃₃₉ (negative control), **b** MPO₄₀₉₋₄₂₈ (positive control), **c** *Treponema vincentii*-derived hypothetical protein, HP₁₆₇₋₁₈₆, **d** *Aspergillus fumigatus*-derived HEAT repeat protein, HRP₈₂₅₋₈₄₄, **e** *Helicobacter pylori*-derived RNA polymerase factor sigma-54, RPF₁₆₃₋₁₈₂, or **f** *Bacteroides* sp.-derived chloramphenicol O-acetyltransferase, COA₁₀₄₋₁₂₃, then, T-cell recall responses measured ex vivo by restimulating draining lymph node cells with either the immunizing peptide, MPO₄₀₉₋₄₂₈ or recombinant mouse MPO (rmMPO) by [³H]-thymidine proliferation assays (top row), and ELISPOT for IFN- γ (middle row) or IL-17A (bottom row). Each dot represents the response from one mouse, error bars are the mean \pm s.e.m. Data are representative of two independent experiments. * $P < 0.05$, ** $P < 0.01$, *** $P < 0.001$ by Kruskal-Wallis test. Source data are provided as a Source Data file

MPO₄₀₉₋₄₂₈ immunized mice using MPO:I-A^b tetramers. Cells were tetramer enriched using magnetic beads, then gated on live, CD4⁺, Dump⁻, MPO:I-A^b tetramer⁺ cells. Compared with naive mice and with mice immunized with OVA₃₂₃₋₃₃₉, mice immunized with 6PGD₃₉₁₋₄₁₀ exhibited a ~30-fold increase in MPO:I-A^b-specific CD4⁺ T cells (Fig. 2b). Thus, 6PGD₃₉₁₋₄₁₀ induces expansion of MPO₄₁₅₋₄₂₅-specific CD4⁺ cells and pro-inflammatory autoreactivity to MPO.

Serum from 6PGD₃₉₁₋₄₁₀ immunized mice bound to fixed thioglycolate induced peritoneal neutrophils from C57BL/6 mice, in a perinuclear ANCA (pANCA) fashion (Fig. 3a) but not to MPO deficient (*Mpo*^{-/-}) mouse neutrophils, and to whole native mouse (nm)MPO by enzyme-linked immune sorbent assay (ELISA) (Fig. 3b), findings that meet the diagnostic criteria for MPO-ANCA positivity in humans³³. Furthermore, purified serum IgG bound to the clinically relevant human linear B-cell epitope MPO₄₄₇₋₄₅₉ (Fig. 3c)³⁴. To demonstrate antibody cross-reactivity between 6PGD₃₉₁₋₄₁₀ and MPO₄₀₉₋₄₂₈, we performed an inhibition ELISA. Purified serum IgG from 6PGD₃₉₁₋₄₁₀ immunized mice was pre-incubated with 6PGD₃₉₁₋₄₁₀, then used to detect anti-MPO₄₀₉₋₄₂₈ IgG by ELISA. Serum IgG from *S. aureus* 6PGD₃₉₁₋₄₁₀ immunized mice pre-incubated with *S. aureus* 6PGD₃₉₁₋₄₁₀ had lower antibody titers compared with serum IgG pre-incubated with blocking buffer only (Fig. 3d). These cross-reacting antibodies were functionally active, as serum IgG from 6PGD₃₉₁₋₄₁₀ immunized mice induced reactive oxygen species production from LPS-primed bone marrow mouse neutrophils in vitro as detected by the conversion of

dihydrorhodamine to rhodamine 123 (Fig. 3e). In vivo, passive transfer of this IgG fraction induced acute neutrophil glomerular recruitment in LPS-primed C57BL/6 mice, albeit at a low level (Fig. 3f). These data demonstrate that antibodies specific for *S. aureus* 6PGD₃₉₁₋₄₁₀ cross-react with MPO₄₀₉₋₄₂₈ and that the *S. aureus*-derived peptide induces both anti-MPO T-cell autoreactivity and biologically active MPO-ANCA.

To identify if the *S. aureus*-derived 6PGD protein is immunoreactive in healthy humans and in AAV patients, we measured IgG antibodies specific for the *S. aureus* pSJH101 6PGD protein by ELISA in sera from a Groningen cohort of healthy human subjects, 31 MPO-AAV patients and 30 PR3-AAV patients. We found detectable levels of *S. aureus* 6PGD-specific IgG in all three groups (Fig. 4a) implying that *S. aureus* pSJH101 6PGD is an immunogenic protein in humans. Furthermore, sera exhibited reactivity to the pSJH101 JH1 *S. aureus* 6PGD₃₉₁₋₄₁₀ sequence by ELISA (Fig. 4b), demonstrating the immunogenicity of this sequence in humans. There were no significant differences in antibody titers between groups. To identify whether 6PGD₃₉₁₋₄₁₀ can cross-react with anti-MPO antibodies in acute MPO-AAV, a Monash cohort of 15 patients with acute, active MPO-AAV was assessed (Supplementary Table 2). Purified IgG from these patients was assessed by inhibition ELISA by pre-incubation with 6PGD₃₉₁₋₄₁₀, then antibodies to human MPO₄₃₅₋₄₅₄ (the homologous sequence to mouse MPO₄₀₉₋₄₂₈) were examined by ELISA. Of the 15 patients, five showed a significant reduction in anti-human MPO₄₃₅₋₄₅₄ titers after incubation with 6PGD₃₉₁₋₄₁₀ (Fig. 4c).

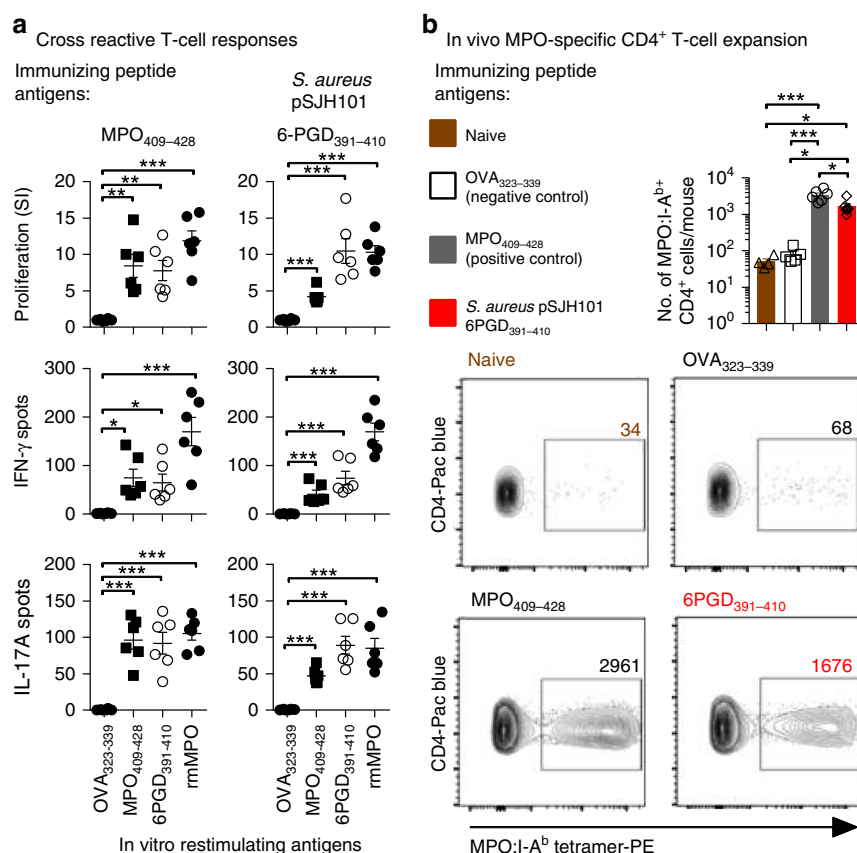


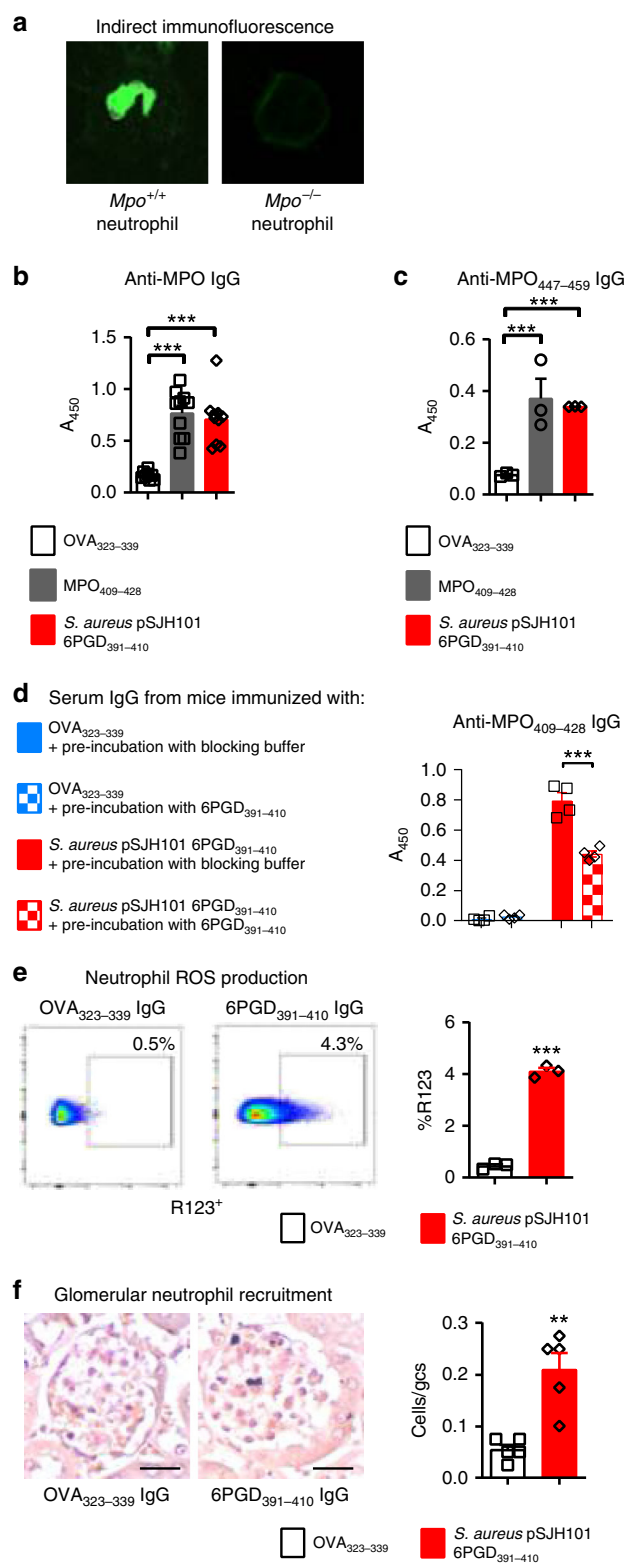
Fig. 2 Immunization with *S. aureus* pSJH101-derived 6PGD₃₉₁₋₄₁₀ induces anti-MPO T-cell responses. **a** C57BL/6 mice ($n = 6$ each group) were immunized with either MPO₄₀₉₋₄₂₈ or *S. aureus* pSJH101-derived 6PGD₃₉₁₋₄₁₀, then T-cell responses measured ex vivo to either OVA₃₂₃₋₃₃₉, MPO₄₀₉₋₄₂₈, 6PGD₃₉₁₋₄₁₀, or recombinant mouse MPO (rmMPO) using [³H]-thymidine proliferation assays (top row), and ELISPOT for IFN-γ (middle row) or IL-17A (bottom row). Each dot represents one mouse; data are representative of two independent experiments. **b** In vivo expansion of MPO-specific CD4⁺ T cells. Cells from lymph nodes and spleen of C57BL/6 mice, either naive ($n = 4$), immunized with OVA₃₂₃₋₃₃₉ ($n = 5$), MPO₄₀₉₋₄₂₈ ($n = 6$) or *S. aureus* pSJH101-derived 6PGD₃₉₁₋₄₁₀ ($n = 6$). Results are expressed as number of MPO:I-A^b tetramer⁺ cells per mouse. Error bars represent the mean \pm s.e.m. * $P < 0.05$, ** $P < 0.01$, *** $P < 0.001$ by Kruskal-Wallis test. Source data are provided as a Source Data file

***S. aureus* clonal specificity for the 6PGD₃₉₇₋₄₀₈ mimotope.** This particular 6PGD₃₉₇₋₄₀₈ sequence is unique to the *Staphylococcus* genus. *S. aureus* makes up the majority of publicly available staphylococcal genomes and the 6PGD₃₉₇₋₄₀₈ sequence of interest predominates in a clinically relevant *S. aureus* clonal complex (CC) known as CC5, to which the JH-1 strain belongs^{35,36}. We assessed the multi-locus sequence type of 136 of the 143 sequenced *S. aureus* strains containing the 6PGD₃₉₇₋₄₀₈ mimic sequence and found that 115 (85% of those typed) of them were CC5. *S. aureus* CC5 strains have been described in Asia, America, Australia, Africa, and Europe³⁵⁻³⁷. There are 2544 publicly available CC5 *S. aureus* genomes, indicating that $\sim 5\%$ of sequenced CC5 strains contain the 6PGD₃₉₇₋₄₀₈ sequence. To assess the specificity of the CC5 related 6PGD₃₉₇₋₄₀₈ sequence in inducing cross-reactivity to MPO, we selected the four 6PGD variants most homologous to the pSJH101-derived *S. aureus* sequence (Supplementary Table 3), commonly found in sequenced *S. aureus* genomes. While each 6PGD peptide induced T-cell reactivity to itself, remarkably, none induced cross-reactive anti-MPO T-cell responses (Fig. 5a-f). Mice immunized with these variants did not develop MPO-ANCA, either by indirect immunofluorescence on mouse neutrophils (Fig. 6a) or by ELISA (Fig. 6b). When we measured anti-MPO₄₄₇₋₄₅₉-specific IgG in purified serum IgG, detectable levels of IgG were found only in Variant 1, but not in any of the other 6PGD peptide variants (Fig. 6c). Therefore, while the variant sequences of this *S. aureus*

6PGD-derived peptide are immunogenic, it is only the JH1, pSJH101 6PGD₃₉₇₋₄₀₈ sequence that induces anti-MPO T-cell responses and MPO-ANCA. To exclude the possibility that the orthologous, but dissimilar mammalian 6PGD sequence (6PGD₃₉₄₋₄₁₃) itself represented a new autoimmune target, mice were immunized with mouse 6PGD₃₉₄₋₄₁₃. This sequence did not induce cross-reactivity to MPO₄₀₉₋₄₂₈ or whole MPO (Supplementary Fig. 1).

Immunization with 6PGD₃₉₁₋₄₁₀ leads to anti-MPO nephritis.

To determine if the loss of tolerance to MPO induced by *S. aureus* JH1-derived pSJH101 6PGD₃₉₁₋₄₁₀ could result in anti-MPO glomerulonephritis, we used our established model of T-cell-mediated anti-MPO glomerulonephritis^{9,38}. In this model, C57BL/6 mice immunized with MPO lose tolerance to MPO but do not develop ANCA of sufficient pathogenicity to induce glomerulonephritis. Therefore, MPO is deposited within the glomerulus via neutrophils transiently recruited by injection of low dose of heterologous anti-mouse basement membrane globulin. In this context, effector MPO-specific T cells recognize MPO peptides and mediate glomerular injury^{6,8,9}. MPO-immunized mice develop glomerulonephritis with pathological albuminuria and segmental glomerular necrosis. Using this protocol, mice immunized with the *S. aureus* JH1-derived pSJH101 6PGD₃₉₁₋₄₁₀ peptide developed glomerulonephritis of similar severity to MPO-



immunized mice with elevated albuminuria, glomerular segmental necrosis, and inflammatory cell infiltrates (Fig. 7). Furthermore, the pSJH101 6PGD₃₉₁₋₄₁₀ immunized mice developed MPO-ANCA and T-cell reactivity to rmMPO, detected by measuring dermal delayed type hypersensitivity to rmMPO. A further group of mice was immunized with the Variant 3 peptide of 6PGD₃₉₁₋₄₁₀ (Supplementary Table 3), chosen because, of the four variants it was found most frequently in sequenced strains of

Fig. 3 MPO-ANCA production in *S. aureus* pSJH101 6PGD₃₉₁₋₄₁₀ immunized mice. **a** Serum IgG from *S. aureus* pSJH101-derived 6PGD₃₉₁₋₄₁₀ immunized C57BL/6 mice (pooled, $n = 8$) binds to neutrophils from C57BL/6 mice, but not those from *Mpo*^{-/-} mice in a perinuclear (pANCA) fashion. **b** Anti-MPO ELISA on sera from mice immunized with OVA₃₂₃₋₃₃₉ ($n = 8$), MPO₄₀₉₋₄₂₈ ($n = 10$), or pSJH101 6PGD₃₉₁₋₄₁₀ ($n = 10$, values representative of two independent experiments). **c** Anti-MPO₄₄₇₋₄₅₉ ELISA using pooled serum IgG from pSJH101 6PGD₃₉₁₋₄₁₀-immunized mice, triplicates representative of two independent experiments. **d** *S. aureus* pSJH101 6PGD₃₉₁₋₄₁₀ inhibits autoantibody binding to MPO₄₀₉₋₄₂₈. Serum IgG from *S. aureus* pSJH101 6PGD₃₉₁₋₄₁₀ immunized mice was pre-incubated with *S. aureus* pSJH101 6PGD₃₉₁₋₄₁₀ then used to detect anti-MPO₄₀₉₋₄₂₈ IgG antibodies by ELISA. Values are quadruplicates. **e** Neutrophil reactive oxygen species (ROS) production via rhodamine 123 (R123) induced by pooled serum IgG from pSJH101 6PGD₃₉₁₋₄₁₀ immunized mice. Flow cytometric plots illustrate the data, performed in triplicate. **f** Glomerular neutrophil recruitment after injection of serum IgG from pSJH101 6PGD₃₉₁₋₄₁₀ immunized mice ($n = 5$ each group). Photomicrographs illustrate the data, presented numerically as neutrophils per glomerular cross section (Cells/gcs). Scale bar is 30 μ m. Error bars represent mean \pm s.e.m. $^{**}P < 0.01$, $^{***}P < 0.001$ by Kruskal-Wallis test (**b, c**), Mann-Whitney *U*-test (**d, e, f**). Source data are provided as a Source Data file

S. aureus. As hypothesized, mice immunized with Variant 3 of 6PGD₃₉₁₋₄₁₀ did not develop disease (Fig. 7), demonstrating the relative specificity of the JH1 pSJH101 6PGD₃₉₁₋₄₁₀ sequence in nephritogenic anti-MPO autoimmunity.

S. aureus JH1 with pSJH101 immunization leads to nephritis.

To address a specific role for the *S. aureus* pSJH101 plasmid-derived 6PGD₃₉₁₋₄₁₀ sequence in anti-MPO autoimmunity and glomerulonephritis in the context of whole bacteria, we immunized mice with either heat-killed *S. aureus* JH1 strain containing the pSJH101 plasmid or heat-killed JH1 that had been cured of the pSJH101 plasmid (Supplementary Fig. 2a) and induced the same model of glomerulonephritis. Compared to mice immunized with cured heat-killed *S. aureus* JH1, mice immunized with *S. aureus* JH1 containing pSJH101 developed glomerulonephritis with pathological albuminuria, glomerular focal, and segmental necrosis and infiltrates of CD4⁺ T cells, CD8⁺ T cells and macrophages (Fig. 8). Mice immunized with *S. aureus* JH1 containing the pSJH101 plasmid also developed MPO-ANCA and MPO-specific secretion of IFN- γ and tumor necrosis factor (TNF) measured in supernatants of cultured splenocytes restimulated with rmMPO (Fig. 8). Therefore, the pSJH101 plasmid containing the cross-reactive *S. aureus* 6PGD sequence is required for anti-MPO cross-reactivity and disease.

Plasmid and strain independent 6PGD induced anti-MPO immunity.

To determine if it is the specific 6PGD sequence that causes disease independent of other proteins encoded by pSJH101 and independent of the *S. aureus* strain, we cloned 6PGD containing the mimic ₃₉₇TDYQEALRDVVA₄₀₈ sequence into the inducible vector pALC2073 (that does not otherwise express 6PGD) to create pALC2073-6PGD. We then transformed a common laboratory *S. aureus* strain (RN4220³⁹, that contains neither plasmids nor 6PGD ₃₉₇TDYQEALRDVVA₄₀₈) with either pALC2073-6PGD or pALC2073 alone. Enhanced expression of 6PGD was confirmed after the induction of anhydrotetracycline (Supplementary Fig. 2b). We immunized mice with heat-killed *S. aureus* RN4220 expressing 6PGD or heat-killed *S. aureus* RN4220 with pALC2073 alone, and disease was again triggered by low-

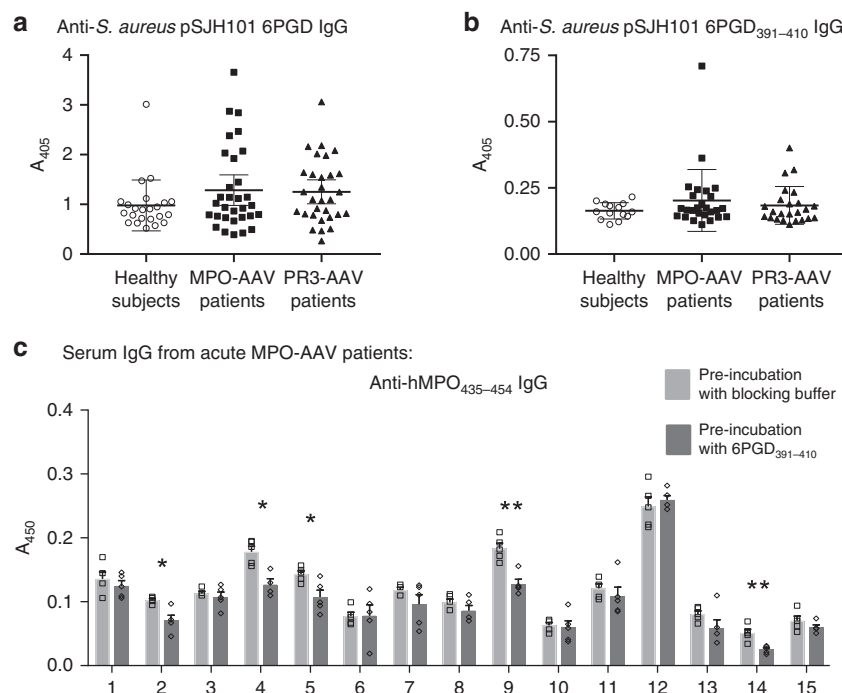


Fig. 4 Humoral responses to 6PGD and *S. aureus* pSJH101 6PGD₃₉₁₋₄₁₀ in humans. **a** Sera from healthy subjects ($n = 23$), MPO-AAV ($n = 31$) and PR3-AAV patients ($n = 30$) assessed by ELISA for pSJH101-derived recombinant 6PGD. **b** Sera from healthy subjects ($n = 14$), MPO-AAV ($n = 26$) and PR3-AAV patients ($n = 24$) assessed by ELISA to pSJH101 6PGD₃₉₁₋₄₁₀. **c** *S. aureus* pSJH101 6PGD₃₉₁₋₄₁₀ inhibits autoantibody binding to human MPO₄₃₅₋₄₅₄ (the MPO₄₀₉₋₄₂₈ homolog) in acute MPO-AAV. Serum IgG from patients with acute MPO-AAV ($n = 15$) were pre-incubated with *S. aureus* pSJH101 6PGD₃₉₁₋₄₁₀ then used to detect anti-hMPO₄₃₅₋₄₅₄ IgG antibodies by ELISA. Values are quintuplicates. Error bars in **a** and **b** are mean \pm s.d., in panel **c** mean \pm s.e.m. * $P < 0.05$, ** $P < 0.01$, Mann-Whitney U -test. Source data are provided as a Source Data file

dose heterologous anti-mouse basement membrane antibodies. Mice immunized with *S. aureus* RN4220 with pALC2073 containing 6PGD developed elevated albuminuria, glomerular segmental necrosis, increases in glomerular CD4⁺ T cells, CD8⁺ T cells and macrophages, as well as MPO-specific IgG and MPO-specific splenocyte secretion of IFN- γ and TNF (Fig. 9). Mice immunized with RN4220 with pALC2073 alone were similar to OVA-immunized mice (Fig. 9). Therefore, it is the 6PGD sequence₃₉₁YFKNIVTDYQEALRDVVATG₄₁₀ itself that induces anti-MPO pathogenic autoreactivity, independent of the *S. aureus* strain or plasmid used.

MHCII promiscuous induction of anti-MPO cross-reactivity.

The dominant MPO T-cell epitope MPO₄₀₉₋₄₂₈, defined in I-A^b expressing C57BL/6 mice is MHCII promiscuous, as MPO₄₀₉₋₄₂₈ also induces autoreactivity in BALB/c mice expressing I-A^d/E^d and in humanized HLA transgenic mice expressing HLA-DR15⁶. Here, we show that the core MPO T-cell epitope, MPO₄₁₅₋₄₂₅, previously defined in C57BL/6 mice is the same in both BALB/c and HLA-DR15 mice (Supplementary Fig. 3a, b) and the critical amino acids, defined by alanine substitution, are similar (Supplementary Fig. 3c). To determine if the pSJH101-derived 6PGD₃₉₁₋₄₁₀ induces anti-MPO cross-reactivity in mice expressing different MHCII molecules, we immunized either BALB/c or humanized HLA-DR15 transgenic mice with 6PGD₃₉₁₋₄₁₀ and measured T-cell reactivity, by [³H]-T proliferation assays and ELISPOT for IFN- γ and IL-17A, to 6PGD₃₉₁₋₄₁₀ itself and cross-reactivity to MPO₄₀₉₋₄₂₈ and to rmMPO. We found that both BALB/c and HLA-DR15 transgenic mice developed immunoreactivity to 6PGD₃₉₁₋₄₁₀, and cross-reactivity both to MPO₄₀₉₋₄₂₈ and to rmMPO (Fig. 10a, b), supporting the notion that pSJH101

6PGD₃₉₁₋₄₁₀ sequence can be effectively presented and induce anti-MPO cross-reactivity by a variety of MHCII alleles.

Discussion

Although we know that a critical step in the development of autoimmune disease is the activation of pro-inflammatory T cells that react with self-antigens, the steps that precipitate the development and activation of these pathogenic T cells are still unclear. Recently, we have shown that peptide register is a key determinant of the phenotype of the autoreactive T-cell repertoire⁴⁰. While molecular mimicry is often flagged as a potential trigger for the activation of existing autoreactive pro-inflammatory T cells, fewer studies have formally demonstrated microbial-self-peptide cross-reactivity, which is often attributable to the lack of understanding of the self-antigen that precipitates disease²⁶⁻²⁸. The current studies not only identify a mimotope peptide, pSJH101 6PGD₃₉₁₋₄₁₀ that induces anti-MPO T and B-cell autoimmunity, they also highlight both the sensitivity of such mimicry, as very similar sequences to the mimic peptide were unable to induce cross-reactivity. Importantly our studies demonstrate the potential for mimicry to be induced by a plasmid-encoded microbial sequence, identifying a potential new role for bacterial plasmids in the pathogenesis of disease.

We and others have identified a “molecular hotspot” within MPO where an immunodominant T-cell epitope and a disease-associated antibody epitope overlap^{6,8,34}. PR3-AAV is classically associated with *S. aureus*^{14,15} and reports also implicate *S. aureus* infections in MPO-AAV¹⁹⁻²². However, despite the presence of neutrophil-derived MPO at sites of infection in a potentially “dangerous” immunological context, the links between the loss of tolerance to MPO and microbial-derived peptides are unclear. Using a standard and unbiased approach of searching microbial

Immunizing peptide antigens:

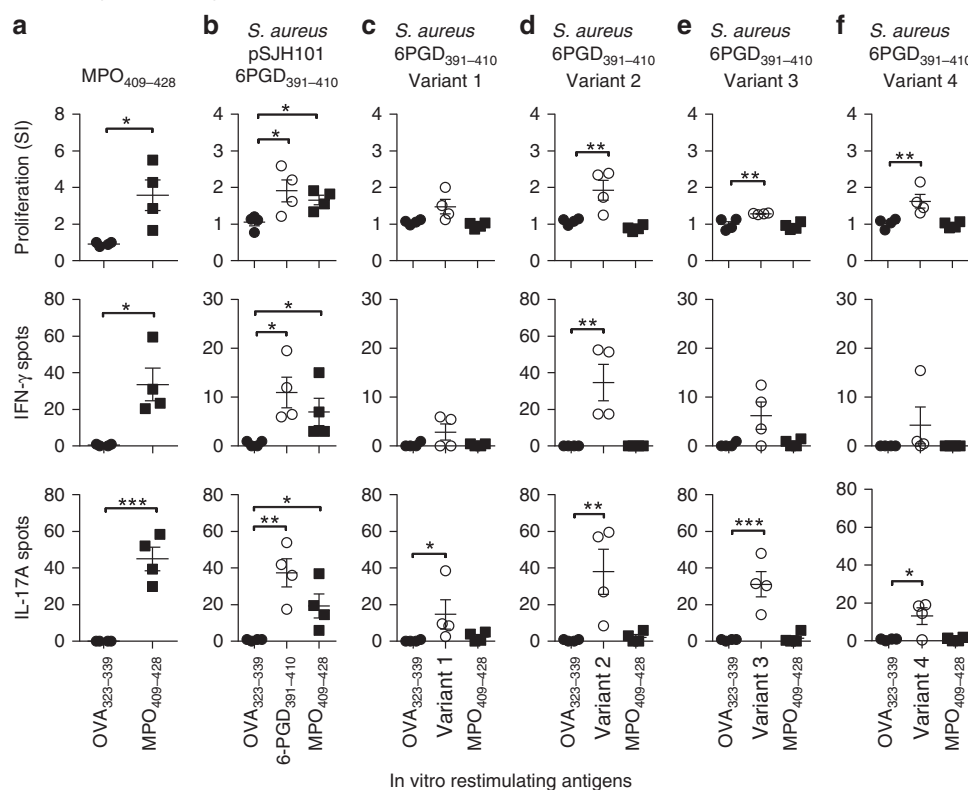


Fig. 5 Anti-MPO T-cell responses after immunization *S. aureus*-derived 6PGD₃₉₁₋₄₁₀ sequences. C57BL/6 mice ($n = 4$ each group) were immunized with either **a** MPO₄₀₉₋₄₂₈ (positive control), **b** pSJH101-derived 6PGD₃₉₁₋₄₁₀ (YFKNIVTDYQEALRDVVATG), **c** *S. aureus* 6PGD₃₉₁₋₄₁₀ Variant 1 (YFKNIVTDYQDALRDVVATG), **d** *S. aureus* 6PGD₃₉₁₋₄₁₀ Variant 2 (YFKNIVTNYQEALRDVVATG), **e** *S. aureus* 6PGD₃₉₁₋₄₁₀ Variant 3 (YFKNIVTEYQDALRDVVATG), **f** *S. aureus* 6PGD₃₉₁₋₄₁₀ Variant 4 (YFKNIVTNYQDALRDVVATG). T-cell recall responses were measured ex vivo to either OVA₃₂₃₋₃₃₉, the immunizing peptide, or MPO₄₀₉₋₄₂₈ using [³H]-thymidine proliferation assays (top row), and ELISPOT IFN-γ (middle row) or IL-17A (bottom row). Each dot represents the response from an individual mouse, error bars represent the mean ± s.e.m. Data are representative of two independent experiments. * $P < 0.05$, ** $P < 0.01$, *** $P < 0.001$ by Kruskal-Wallis test. Source data are provided as a Source Data file

proteomes in silico for peptide sequences with the highest sequence similarities to MPO₄₄₁₋₄₅₁ we identified a number of microbial peptides from human pathogens, but experimentally these sequences did not induce anti-MPO cross-reactivity. However, when *S. aureus*-derived peptides sharing the critical amino acid residues were examined, we identified a plasmid-derived peptide that induces anti-MPO immunoreactivity in the context of several different MHCII molecules and that is immunogenic in humans.

This MPO mimotope, pSJH101 6PGD₃₉₁₋₄₁₀, is overall less homologous than the other non-cross-reactive microbial-derived peptides tested, demonstrating that sequence similarity itself is not necessarily a predictor of molecular mimicry⁴¹. Instead, specific structural determinants may be more of a contributory factor that leads to cross-reactivity⁴². Our experiments, using similar 6PGD₃₉₁₋₄₁₀ sequences from a range of *S. aureus* strains demonstrated that even single amino-acid substitutions were sufficient to abrogate anti-MPO cross-reactivity. For example, in Variant 1, a substitution from glutamic acid (E) to the smaller aspartic acid (D), and in Variant 2, a substitution from the negatively charged aspartic acid (D) to the uncharged asparagine (N), prevented the induction of anti-MPO cross-reactivity, highlighting the exquisite sensitivity of TCRs to specific peptide structures.

Using ex vivo restimulation assays, as well as MPO:I-A^b tetramers, we have demonstrated that pSJH101 6PGD₃₉₁₋₄₁₀ can

induce anti-MPO CD4⁺ T-cell cross-reactivity. Furthermore, in addition to cellular immunity, the 6PGD₃₉₁₋₄₁₀ peptide also induces autoantibodies to whole nmMPO, to the disease-associated linear MPO peptide and to an overlapping linear MPO peptide. The 6PGD₃₉₁₋₄₁₀ mimotope inhibited autoantibody binding to this peptide in mice via a solid phase competitive ELISA. 6PGD₃₉₁₋₄₁₀ also inhibited binding to human MPO₄₃₅₋₄₅₄ (equivalent to mouse MPO₄₀₉₋₄₂₈) in 5/15 (33%) of humans with acute MPO-AAV. Collectively, these data confirm a functional interaction between these overlapping epitopes. Thus, the pSJH101 6PGD₃₉₁₋₄₁₀ peptide cross reacts with an MPO T-cell epitope, but it is also likely to be relevant to these linked B-cell epitopes. While it is possible that antibodies to 6PGD₃₉₁₋₄₁₀ serve as effectors, as for example in the seminal studies of Kaplan and Meyesian, and others for streptococcal antigens and acute rheumatic fever^{43,44}, we suggest that this type of direct reactivity at an effector level is less likely in MPO-AAV. Cross-reactivity at a B cell/B-cell receptor level is more likely to be relevant to the promotion of B-cell autoreactivity via binding of 6PGD₃₉₁₋₄₁₀ to the B-cell receptor of potentially autoreactive B cells. This would promote autoreactive anti-MPO B-cell activation by autoreactive CD4⁺ T cells reacting to the same peptide. In this context, the relative affinities of 6PGD₃₉₁₋₄₁₀ and MPO₄₀₉₋₄₂₈ (in humans MPO₄₃₅₋₄₅₄) to anti-MPO antibodies and whether 100% inhibition occurs, is unlikely to be of critical importance. Furthermore, 6PGD₃₉₁₋₄₁₀ alone is unlikely to have a measurable effect on the

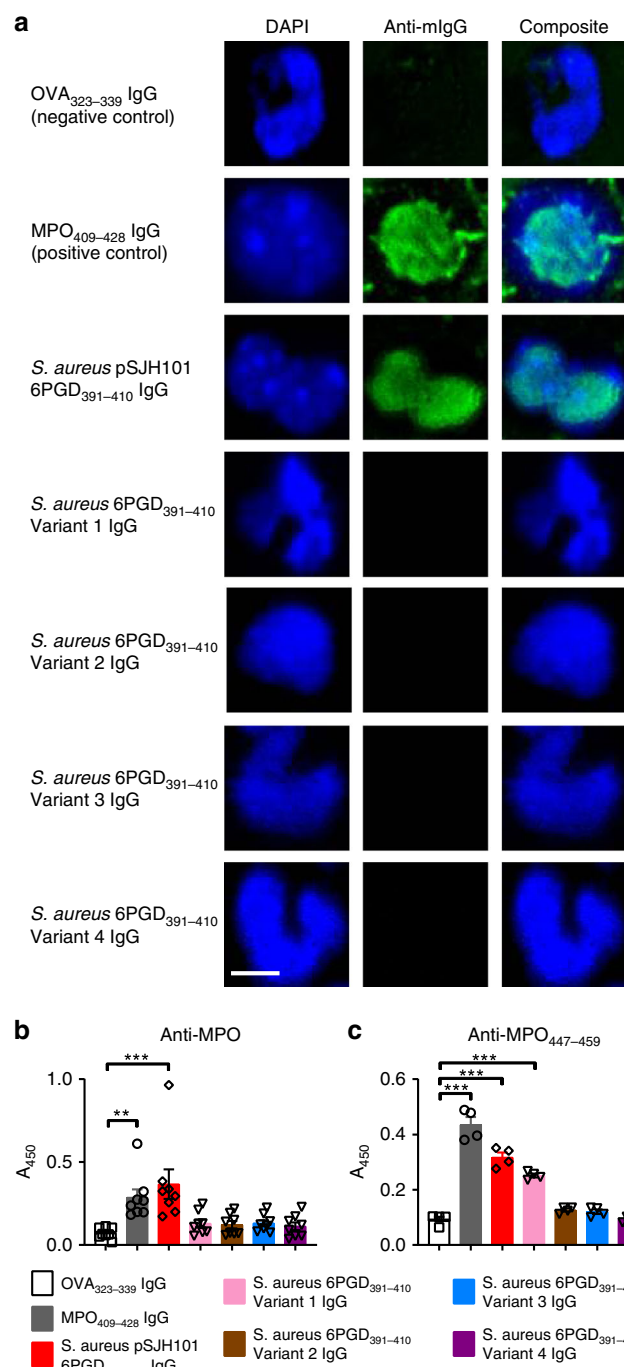


Fig. 6 MPO-ANCA after immunization with *S. aureus*-derived 6PGD₃₉₁₋₄₁₀ sequences. **a** Perinuclear (pANCA) detection using purified serum IgG, pooled from each group of C57BL/6 mice ($n = 8$ each group) immunized with OVA₃₂₃₋₃₃₉, MPO₄₀₉₋₄₂₈, pSJH101-derived 6PGD₃₉₁₋₄₁₀ (YFKNIIVTDYQEALRDVVATG), *S. aureus* 6PGD₃₉₁₋₄₁₀ Variant 1 (YFKNIIVTDYQDALRDVVATG), *S. aureus* 6PGD₃₉₁₋₄₁₀ Variant 2 (YFKNIIVTDYQDALRDVVATG), *S. aureus* 6PGD₃₉₁₋₄₁₀ Variant 3 (YFKNIIVTDYQDALRDVVATG), *S. aureus* 6PGD₃₉₁₋₄₁₀ Variant 4 (YFKNIIVTDYQDALRDVVATG) (amino acid substitutions underlined). Nuclei are blue (DAPI), mouse IgG is green (FITC-conjugated anti-mouse IgG antibody). **b** Sera from individual mice ($n = 8$ each group) immunized with pSJH101-derived 6PGD₃₉₁₋₄₁₀ and other *S. aureus*-derived sequences of 6PGD₃₉₁₋₄₁₀ tested by an anti-rmMPO ELISA. **c** Anti-MPO₄₄₇₋₄₅₉ antibody detection by ELISA using purified serum IgG pooled from each group of C57BL/6 mice (**a**). Scale bar is 5 μ m (all photomicrographs). Error bars represent the mean \pm s.e.m. of triplicates. $^{**}P < 0.01$, $^{***}P < 0.001$ by Kruskal-Wallis test. Source data are provided as a Source Data file

It is not yet known in humans whether carriage or infection of *S. aureus* strains containing the cross-reactive 6PGD₃₉₁₋₄₁₀ sequence promotes the induction of MPO-AAV or precipitates disease relapse. The conditions for 6PGD₃₉₁₋₄₁₀ recognition to induce anti-MPO T-cell cross-reactivity may include *S. aureus* infection, intermittent colonization or chronic colonization. Furthermore, while nasal swabs are the most common way of screening for *S. aureus*, carriage also occurs on the skin, and in the throat, vagina, anus, and lower gastrointestinal tract⁴⁶⁻⁴⁸. It is unlikely that the 6PGD₃₉₁₋₄₁₀ mimotope is the sole factor that determines loss of tolerance to MPO, given the frequency of antibodies to the 6PGD protein and peptide, and the multiple genetic and environmental factors that contribute to the development of MPO-AAV.

Although our data do not conclusively prove a role for 6PGD₃₉₁₋₄₁₀, they suggest that exposure to certain *S. aureus* strains may be a precipitating factor in the loss of tolerance to MPO and the development of MPO-AAV. Our data also demonstrates that plasmids, acting as mobile genetic elements, may transfer a tendency to autoreactivity. The transfer of antibiotic resistance via plasmids is well known. However, the horizontal gene transfer of the cross-reactive 6PGD that we emulated by transforming *S. aureus* RN4220 with pALC2073-6PGD demonstrates that plasmids harboring cross-reactive peptide sequences can induce loss of tolerance. In conclusion, our findings identify pSJH101 6PGD₃₉₁₋₄₁₀ as an MPO cross-reactive mimotope peptide. 6PGD₃₉₁₋₄₁₀ is part of a protein that is immunogenic in humans, can induce loss of tolerance to MPO and experimental anti-MPO glomerulonephritis and MPO-AAV. This sequence is derived from a plasmid found in only some strains of *S. aureus*, implicating plasmid-derived antigens in the loss of tolerance to self-antigens.

Methods

Mice. C57BL/6 and BALB/c mice were obtained from the Monash Animal Research Platform, Clayton, Monash University. *Mpo*^{-/-} mice⁴⁹ and HLA-DR15 Tg⁵⁰ mice were bred at the Monash Medical Center Animal Facility (MMCAF), Monash Medical Center, Clayton. Mice were housed in the SPF facilities at MMCAF and experiments were conducted in male mice aged 6–10 week. All animal studies were approved by the Monash University Animal Ethics Committee (Committee MMCB) and complied with the Australian code for the care and use of animals for scientific purposes (2013).

Human samples. Serum samples from AAV patients and healthy subjects (HS) were obtained from an existing collection of the 'Groningen cohort of AAV', and sera and plasma exchange effluent from Monash patients with acute MPO-AAV were obtained from the Monash Vasculitis Registry and Biobank. Institutional review board (IRB) approval was previously obtained from the Medical Ethics

binding of MPO-ANCA to neutrophils by indirect immunofluorescence, as there are known to be multiple B-cell epitopes in active MPO-AAV³⁴.

There have been several studies of nasal carriage of *S. aureus* in people with PR3-AAV, due in part to sinonasal disease being common in PR3-AAV^{14,15,19}. However, the potential relationship between *S. aureus* and MPO-AAV has been largely unexplored, though colonization with *S. aureus* does occur in patients with this disease¹⁹. Most *S. aureus* strains known to carry the nephritogenic 6PGD₃₉₁₋₄₁₀ sequence belong to the CC5 clonal complex¹⁹. In *S. aureus* carriers with established MPO-AAV, 11% of isolates were CC5 (healthy controls 5%, PR3-AAV 15%)¹⁹. CC5 is a globally distributed clonal complex of *S. aureus* found in both community and hospital settings^{35,36,45}.

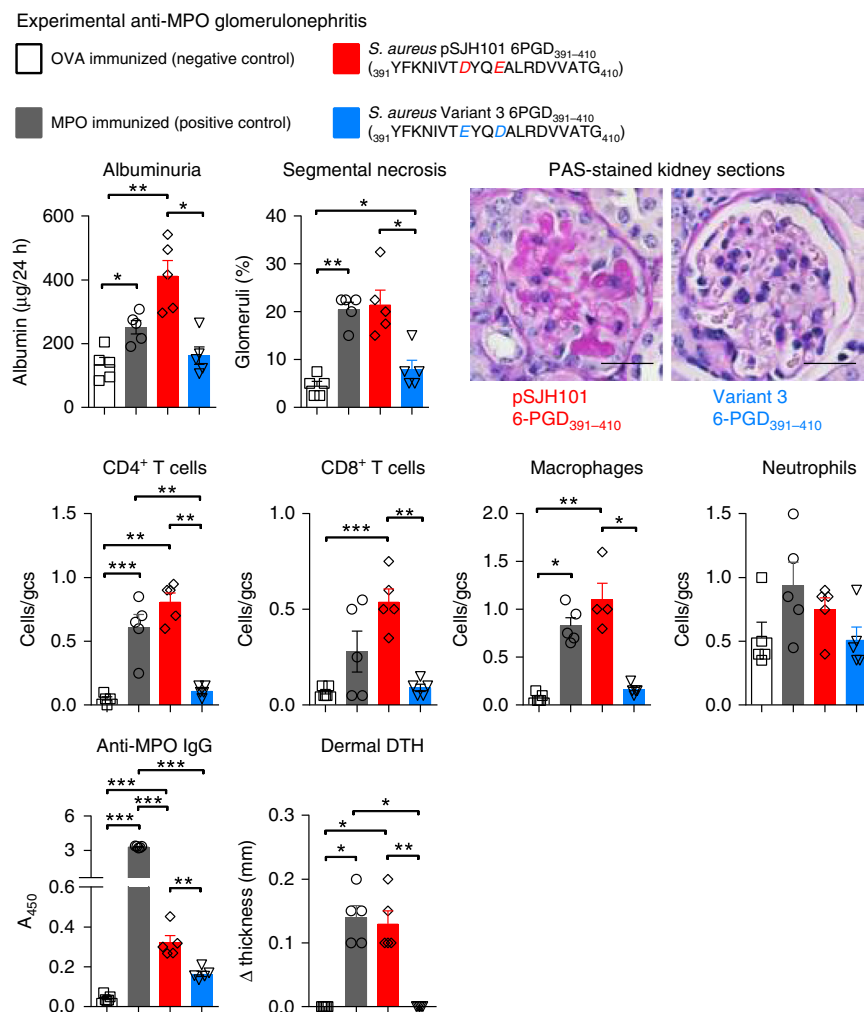


Fig. 7 Experimental anti-MPO glomerulonephritis in *S. aureus* pSJH101 6PGD₃₉₁₋₄₁₀ immunized mice. C57BL/6 mice ($n = 5$ each group) were immunized with either OVA (negative control), MPO (positive control), *S. aureus* pSJH101 6PGD₃₉₁₋₄₁₀ or the common *S. aureus* 6PGD₃₉₁₋₄₁₀ variant, Variant 3. Low-dose heterologous anti-basement membrane globulin was injected intravenously to induce transient neutrophil recruitment and MPO deposition in glomeruli. Glomerular injury was measured by albuminuria, and by glomerular segmental necrosis on periodic acid-Schiff (PAS) stained kidney sections. Photomicrographs glomeruli from *S. aureus* pSJH101 6PGD₃₉₁₋₄₁₀ or *S. aureus* Variant 3 6PGD₃₉₁₋₄₁₀ immunized mice. Inflammatory cells within glomeruli were enumerated and expressed as cells per glomerular cross section (gcs). Anti-MPO autoreactivity determined by detection of anti-MPO IgG by ELISA and dermal delayed type hypersensitivity (DTH) swelling after recombinant mouse MPO intradermal challenge. Scale bar is 30 μ m. Error bars represent the mean \pm s.e.m. * $P < 0.05$, ** $P < 0.01$, *** $P < 0.001$ by Kruskal-Wallis test. Source data are provided as a Source Data file

Committee of the University Medical Center Groningen and the Monash Health Human Research Ethics Committee, respectively. Written informed consent was obtained from all patients and HS, and all experiments were conducted in accordance with the guidelines of the Declaration of Helsinki. All patients fulfilled the Chapel Hill Consensus Conference definitions for the diagnosis of AAV. All patient samples were confirmed positive for either MPO-ANCA or PR3-ANCA by capture ELISA and indirect immunofluorescence on ethanol fixed neutrophils^{51,52}.

Peptides and proteins. All peptides were synthesized at $> 95\%$ purity, confirmed by HPLC (Mimotopes). The residue numbers, in subscript, and peptide sequences, in brackets, of the peptides used are: mouse MPO₄₀₉₋₄₂₈ peptide (PRWNGEK-LYQEARKIVGAMV), *Treponema vincentii* hypothetical protein₁₆₇₋₁₈₆ (LRKQLKRLYKEARKIQKICP), *Aspergillus fumigatus* HEAT repeat protein₈₂₅₋₈₄₄ (ISALPQRWYQEARKIIEFAA), *Helicobacter pylori* RNA polymerase factor sigma-54₁₆₃₋₁₈₂ (RELDNNELYEEARKIILNLE), *Bacteroides* sp. chloramphenicol O-acetyltransferase₁₀₄₋₁₂₃ (YHEDFETFFYQEARKIIDSIP), *S. aureus* pSJH101-derived 6PGD₃₉₁₋₄₁₀ (YFKNIVTDYQ³⁹¹ALRDVVATG), *S. aureus* 6PGD₃₉₁₋₄₁₀ Variant 1 (YFKNIVTDYQ³⁹¹DALRDVVATG), *S. aureus* 6PGD₃₉₁₋₄₁₀ Variant 2 (YFKNIVTDYQ³⁹¹ALRDVVATG), *S. aureus* 6PGD₃₉₁₋₄₁₀ Variant 3 (YFKNIVTDYQ³⁹¹DALRDVVATG), *S. aureus* 6PGD₃₉₁₋₄₁₀ Variant 4 (YFKNIVTDYQ³⁹¹DALRDVVATG), *Mus musculus* 6PGD₃₉₄₋₄₁₃ (FFKSAVDNQCQDSWRRVIS TGV), and control OVA₃₂₃₋₃₃₉ peptide (ISQAVHAAHAEINEAGR). Sequences of

the shortened MPO peptides are listed in Supplementary Table 3. Immunizations to induce CD4⁺ T-cell responses were performed with 20-mers containing the core 11 amino acids because MHC class II molecules have open-ended binding pockets and additional amino acids on either side enhances immunoreactivity⁶. MPO was produced using a baculovirus system⁵³ and OVA was purchased (Sigma-Aldrich). Recombinant *S. aureus* pSJH101 6PGD (Genbank ID: CP000737.1) (GeneArt®, ThermoFisher Scientific) was produced using the Champion pET101 Directional TOPO Expression Kit with BL21 Star (DE3) One Shot chemically competent *E. coli* (ThermoFisher Scientific). Expression was confirmed by using anti-V5 monoclonal antibodies by western blotting and purified by 6xHis tag elution using nickel resins (Promega).

Generation of MPO:I-A^b tetramers. MHCII monomers were produced in High Five insect cells (*Trichoplusia ni* BTI-Tn-5B1-4 cells, Invitrogen) using the baculovirus expression system^{40,54,55}. DNA encoding the I-A^b α - and β -chains and the mouse MPO₄₁₅₋₄₂₈ (415KLYQEARKIVGAMV₄₂₈), fused to the N-terminus of the β -chain via a flexible linker (SGGSGSGSAS), were cloned into pFastBac Dual vector and recombinant baculovirus propagated in Sf9 insect cells (*Spodoptera frugiperda*, Invitrogen). The C-termini of the I-A^b α - and β -chains contained enterokinase cleavable Fos and Jun leucine zippers, respectively, to promote correct heterodimeric pairing. The C-terminus of the β -chain also contained a BirA ligase recognition sequence for biotinylation and poly-histidine tag for purification,

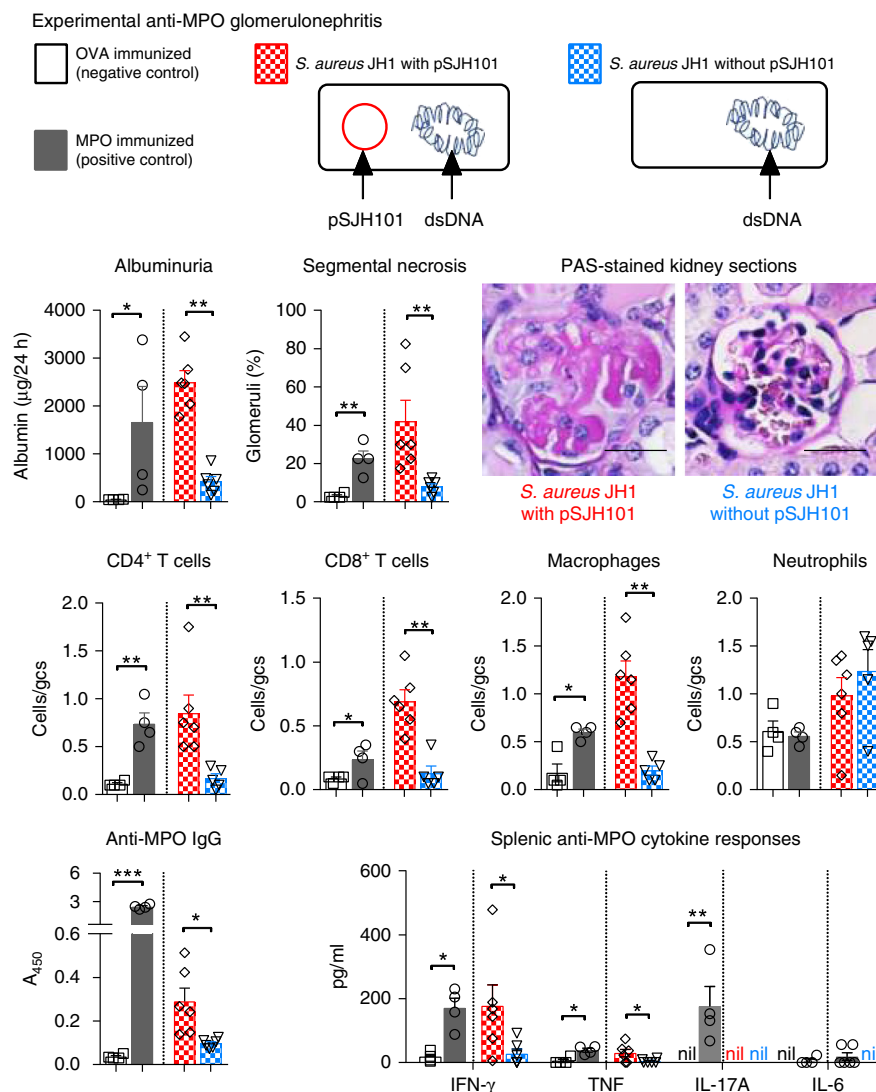


Fig. 8 Experimental anti-MPO glomerulonephritis in mice injected with *S. aureus* containing pSJH101 6PGD₃₉₁₋₄₁₀. C57BL/6 mice were immunized with either OVA (negative control, $n = 4$), MPO (positive control, $n = 4$), *S. aureus* JH1 with pSJH101 ($n = 6$) or cured *S. aureus* JH1 without pSJH101 ($n = 6$). OVA and MPO were emulsified in Freund's complete adjuvant; *S. aureus* JH1 with or without pSJH101 were emulsified in Titermax. MPO was deposited in glomeruli using heterologous low-dose anti-basement membrane globulin. Glomerular injury was measured by albuminuria, and by glomerular segmental necrosis on periodic acid-Schiff (PAS) stained kidney sections. Photomicrographs depict glomeruli from mice immunized with either *S. aureus* JH1 with pSJH101 or *S. aureus* JH1 without pSJH101. Inflammatory cells within glomeruli were enumerated and expressed as cells per glomerular cross section (gcs). Anti-MPO autoreactivity determined by detection of anti-MPO IgG by ELISA and by measuring inflammatory cytokines, IFN- γ , TNF, IL-17A, and IL-6 in recombinant mouse MPO stimulated splenocyte cultures. Scale bar is 30 μm . Error bars represent the mean \pm s.e.m. * $P < 0.05$, ** $P < 0.01$, *** $P < 0.001$ by Mann-Whitney U -test. Source data are provided as a Source Data file

immediately following the Jun leucine zipper sequence. MPO:I-A^b monomers were purified from baculovirus infected High Five insect cell supernatants through immobilized metal ion affinity (Ni Sepharose 6 Fast-Flow, GE Healthcare), size exclusion (S200 Superdex 16/600, GE Healthcare) and anion exchange (HiTrap Q, HP, GE Healthcare) chromatography. MPO:I-A^b tetramers were assembled by the addition of Streptavidin-PE (BD Biosciences)^{54,55}.

Plasmids and *Staphylococcus aureus* strains. The pSJH101 plasmid was found within a clinical isolate of *S. aureus* JH1 (also known as strain A8090)⁵⁶. To cure the pSJH101 plasmid from *S. aureus* JH1, cells were cultured with 0.004% SDS at 45 °C for 24 h⁵⁷. To confirm the presence or absence of the pSJH101 plasmid containing 6PGD, PCR was performed on cell lysates using primers specific for: *cls2*, forward primer 5' GCAAGGTACCATGATAGAGTTATTATCCATTGC 3', reverse primer 5' GCAAGAGCTCTTAGTGTTGATGTTGATGATGTAAGATAGGTGACAATAATTGTG 3'; pSJH101, forward primer 5' CATTGGCGAATCAACAACAC 3', reverse primer 5' ACTCCACTTTTGGGGGAAC 3'; and the pSJH101-derived 6PGD, which do not amplify the more common 6PGD (Variant 3) present in the

chromosomal DNA of JH1: forward primer 5'TCATCATCTAACAGCGGAAGT3' and reverse primer 5' ACCCCGTAAAAATTTTGTGAT 3'.

The 6PGD sequence (derived from pSJH101) was cloned into the tetracycline inducible pALC2073 plasmid⁵⁸. *S. aureus* RN4220, which contains neither plasmids nor the 6PGD₃₉₇TDYQEALRDVVA₄₀₈ sequence, was transformed by electroporation with either pALC2073 containing 6PGD or pALC2073 without 6PGD^{59,60}. To confirm expression of 6PGD we performed PCR on cDNA from cultured *S. aureus* RN4220 containing pALC2073 with 6PGD with or without tetracycline, *S. aureus* RN4220 containing pALC2073 without 6PGD cultured with tetracycline. As a control for specificity, we performed PCR using chromosomal DNA of *S. aureus* RN4220. The primers we used were: forward primer 5' TCATCACTAACAGCGGAAGT 3' and reverse primer 5' ACCCCGTAAAAATTTTGTGAT 3'. The primers we used were: forward primer 5' TCATCATCTAACAGCGGAAGT 3' and reverse primer 5' ACCCCGTAAAAATTTTGTGAT 3'. For in silico multi-locus sequence typing (MLST), the software *mlst* was used to identify the sequence types (STs) after scanning the genomes of interest⁶¹, then STs were grouped into CC in which each ST in the CC shares at least six identical alleles of the seven loci with at least one other member of the group⁶².

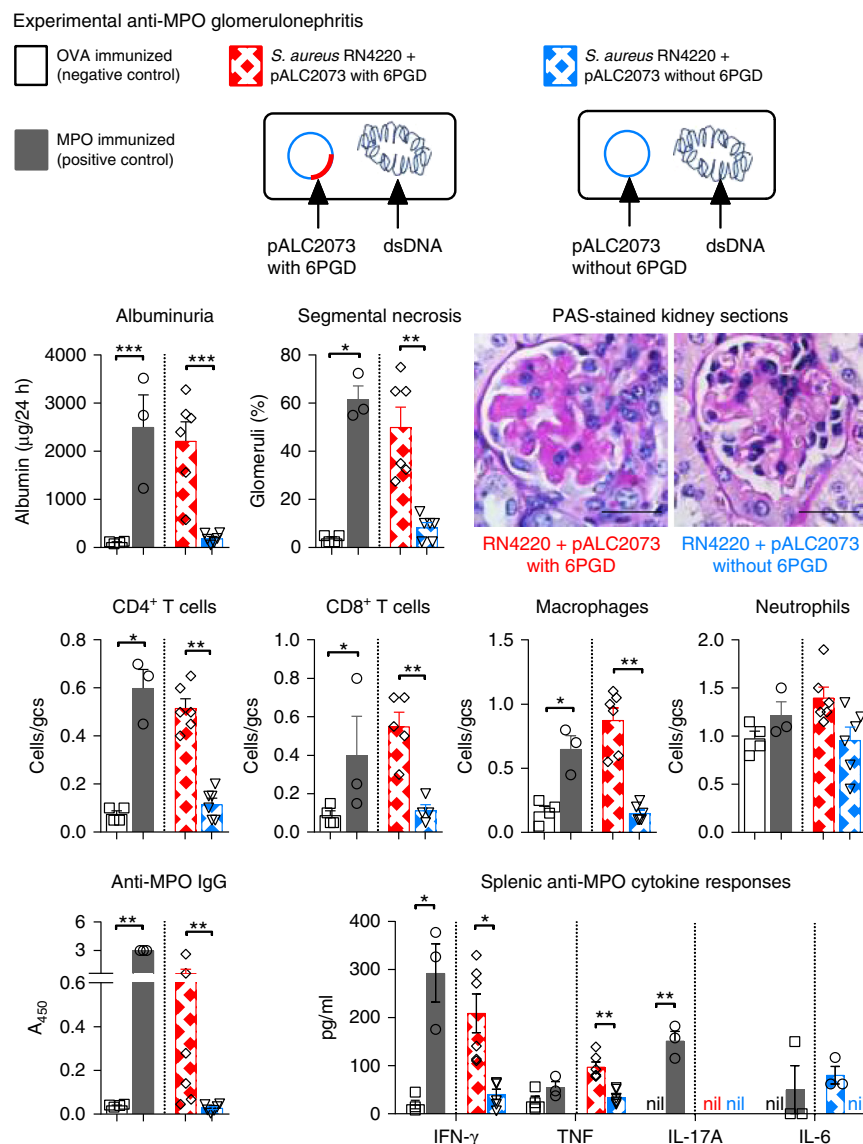


Fig. 9 Experimental anti-MPO glomerulonephritis in mice injected with *S. aureus* RN4220 containing pALC2073. C57BL/6 mice were immunized with either OVA (negative control, $n = 4$), MPO (positive control, $n = 3$), *S. aureus* RN4220 containing pALC2073 with 6PGD ($n = 6$) or *S. aureus* RN4220 containing pALC2073 alone, without 6PGD ($n = 6$). OVA and MPO were emulsified in Freund's complete adjuvant; *S. aureus* RN4220 containing pALC2073 with or without 6PGD were emulsified in Titermax. MPO was deposited in glomeruli using heterologous low-dose anti-basement membrane globulin. Renal injury was measured by albuminuria, and by glomerular segmental necrosis on periodic acid-Schiff (PAS) stained kidney sections. Photomicrographs depict glomeruli from mice immunized with either *S. aureus* RN4220 containing pALC2073 with 6PGD or RN4220 containing pALC2073 without 6PGD. Inflammatory cells within glomeruli were enumerated and expressed as cells per glomerular cross section (gcs). Anti-MPO autoreactivity determined by detection of anti-MPO IgG by ELISA and by measuring inflammatory cytokines, IFN- γ , TNF, IL-17A, and IL-6 in recombinant mouse MPO stimulated splenocyte cultures. Scale bar is 30 μm . Error bars represent the mean \pm s.e.m. * $P < 0.05$, ** $P < 0.01$, *** $P < 0.001$ by Mann-Whitney U -test. Source data are provided as a Source Data file

Induction and assessment of T-cell responses. Mice were immunized with 10 μg of peptide emulsified in Freund's complete adjuvant (FCA) subcutaneously at the base of the tail. Ten days later, draining lymph node cells were isolated and cultured in $[\text{H}]$ -T proliferation assays and/or IFN- γ and IL-17A ELISPOTs. Lymph node cells were cultured in triplicate in supplemented RPMI media (10% vol/vol FCS, 2 mM L-glutamine, 100 U mL^{-1} penicillin, 0.1 mg mL^{-1} streptomycin, 50 μM 2-Mercaptoethanol) at 5×10^5 cells per well in the presence or absence of peptide ($10 \mu\text{g mL}^{-1}$) or whole protein antigen ($10 \mu\text{g mL}^{-1}$) in a humidified incubator at 37 $^{\circ}\text{C}$, 5% CO_2 for 72 h in proliferation assays and 18 h in ELISPOTs. In proliferation assays, $[\text{H}]$ -thymidine was added during the last 16 h of culture and results expressed as a stimulation index. For IFN- γ and IL-17A ELISPOTs (eBioscience, anti-IFN- γ antibodies 551216, 1:250 and 554410, 1:250; anti-IL-17A antibodies 555068, 1:1000 and 555067, 1:1000), spots were developed according to the manufacturer's protocol and results expressed as the mean number of spots minus baseline (media alone). To determine the in vivo expansion of MPO-specific cells,

mice were first immunized with 10 μg of peptide emulsified in FCA subcutaneously at the base of the tail, then, 7 days later, the inguinal, axillary, brachial, cervical, mesenteric, and periaortic lymph nodes and spleen were harvested. Following, tetramer-based magnetic enrichment^{63,64}, cells were incubated with Live/Dead fixable Near IR Dead Cell Stain (Thermo Scientific) then stained with anti-mouse CD4-Pacific Blue (BioLegend, 100531, 1:400) and "dump" antibodies anti-mouse CD11c (all BioLegend, 117311, 1:100), CD11b (101217, 1:100), F4/80 (123120, 1:100), CD8a (100723, 1:100), B220-Alexa Fluor 488 (103225, 1:100). The MPO:I-A^b tetramer⁺ gate was set based on the CD4⁺ live lymphocyte population (see Supplementary Fig. 4 for gating strategy).

Induction and assessment of anti-MPO antibody responses. C57BL/6 mice were immunized with 10 μg of either OVA₃₂₃₋₃₃₉, MPO₄₀₉₋₄₂₈, *S. aureus* pSJH101-derived 6PGD₃₉₁₋₄₁₀, *S. aureus* Variant 1 6PGD₃₉₁₋₄₁₀, *S. aureus* Variant 2

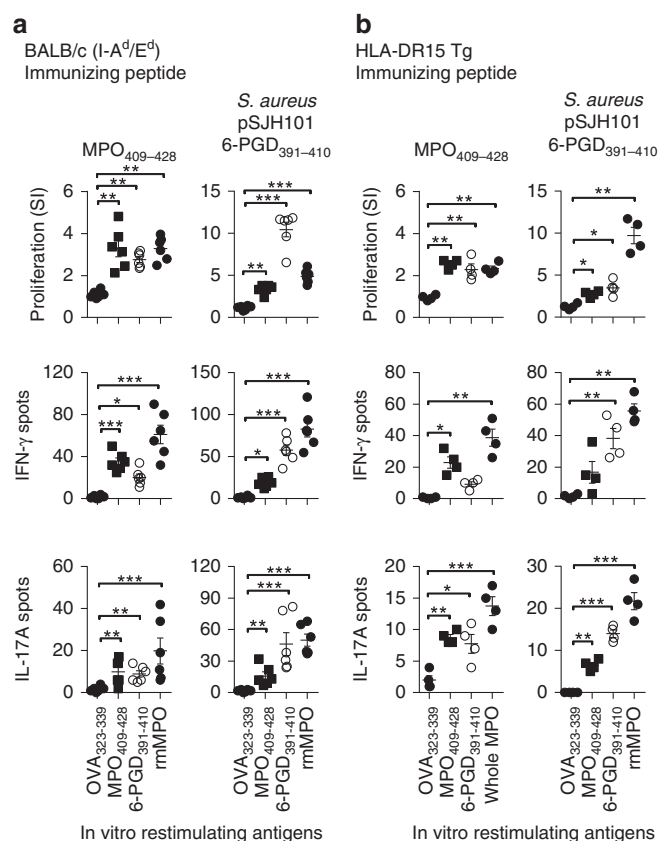


Fig. 10 Anti-MPO T-cell responses in other *S. aureus* pSJH101 6PGD₃₉₁₋₄₁₀ immunized mouse strains. **a** BALB/c (I-A^d/I-E^d) expressing, $n = 6$) and **b** HLA-DR15 transgenic (Tg, $n = 4$) mice were immunized with MPO₄₀₉₋₄₂₈ (positive control) and pSJH101 6PGD₃₉₁₋₄₁₀, then T-cell responses measured ex vivo to either OVA₃₂₃₋₃₃₉ (negative control), MPO₄₀₉₋₄₂₈, 6PGD₃₉₁₋₄₁₀, and recombinant mouse MPO using [³H]-thymidine proliferation assays (top row), and ELISOPT for IFN- γ (middle row) or IL-17A (bottom row). Each dot represents the response from an individual mouse, error bars represents the mean \pm s.e.m. Data are representative of two independent experiments. * $P < 0.05$, ** $P < 0.01$, *** $P < 0.001$ by Kruskal-Wallis test. Source data are provided as a Source Data file

6PGD₃₉₁₋₄₁₀, *S. aureus* Variant 3 6PGD₃₉₁₋₄₁₀ or *S. aureus* Variant 4 6PGD₃₉₁₋₄₁₀; first on day 0 emulsified in (FCA), then boosted on days 7 and 14 emulsified in Freund's incomplete adjuvant (FIA). Serum was collected from mice by cardiac puncture on day 28 and Protein G purified for indirect immunofluorescence on ethanol fixed neutrophils. Thioglycolate induced peritoneal neutrophils were obtained from either *Mpo*^{+/+} or *Mpo*^{-/-} C57BL/6 mice, cytospun onto glass slides then ethanol fixed^{6,33}. Pooled serum IgG was incubated with slides for 1 h, then anti-mouse IgG detected using a chicken anti-mouse Alexa Fluor 488 secondary antibody (Molecular Probes, A-21200, 1:200). DAPI was used as a nuclear stain and fluorescence detected by either fluorescence microscopy or confocal microscopy.

ELISAs for anti-MPO and anti-6PGD antibodies. Serum was collected from mice by cardiac puncture on day 28 and either used for the detection of anti-MPO IgG antibodies, anti-MPO₄₄₇₋₄₅₉ IgG antibodies by ELISA and inhibition ELISAs for the detection of anti-MPO₄₀₉₋₄₂₈ IgG antibodies. The anti-MPO IgG ELISA was performed on rmMPO coated, 2% casein/PBS blocked 96-well plates. Anti-MPO₄₄₇₋₄₅₉ IgG ELISA was performed on MPO₄₄₇₋₄₅₉ coated, 2% casein/PBS blocked 96-well plates. Serum (diluted 1:50 in PBS) or pooled IgG (100 μ g ml⁻¹ in PBS) was incubated for 16 h at 4 °C, then anti-mouse IgG detected using a horseradish peroxidase (HRP) conjugated secondary antibody (Amersham, NA-931, 1:2000). For inhibition ELISA, serum IgG (10 μ g ml⁻¹) was pre-incubated with *S. aureus* pSJH101-derived 6PGD₃₉₁₋₄₁₀ on a 96-well ELISA plate (coating concentration 10 μ g ml⁻¹), then transferred to an MPO₄₀₉₋₄₂₈ coated (10 μ g ml⁻¹) 96-well ELISA plate.

Human sera were tested for reactivity to 6PGD (HS $n = 23$, MPO-AAV $n = 31$ and PR3-AAV $n = 30$) and to *S. aureus* pSJH101 6PGD₃₉₁₋₄₁₀ (HS $n = 14$, MPO-AAV $n = 26$) and PR3-AAV patients ($n = 24$) by ELISA. The HS groups were different between assays, and not all samples assayed for whole 6PGD were available for the *S. aureus* pSJH101 6PGD₃₉₁₋₄₁₀ assay. ELISA plates (NUNC Maxisorp, Thermo Fisher Scientific, Breda, The Netherlands) were coated with 100 μ l of 5 μ g ml⁻¹ recombinant *S. aureus* pSJH101 6PGD or 10 μ g ml⁻¹ *S. aureus* pSJH101 6PGD₃₉₁₋₄₁₀ peptide diluted in 0.1 M carbonate-bicarbonate buffer (pH 9.6) overnight. Plates were washed with PBS pH 7.4 with 0.05% Tween-20 and incubated for 1 h at room temperature (RT) with 200 μ l 2% bovine serum albumin (BSA)/PBS per well to prevent non-specific binding. Next, plates were incubated with 100 μ l serum samples (1:50 in PBS 1% BSA, 0.05% Tween-20, 2 h at RT). After washing, plates were incubated with alkaline phosphatase goat anti-human IgG (Sigma, St. Louis, USA, A-5403, 1:1000) for one hour at RT and p-nitrophenyl-phosphate disodium (Sigma) was used as a substrate. Absorbance was measured at 405 nm. For inhibition ELISA, IgG purified from sera or plasma exchange effluent (50 μ g ml⁻¹) was first pre-incubated with *S. aureus* pSJH101-derived 6PGD₃₉₁₋₄₁₀ on a 96-well ELISA plate (coating concentration 10 μ g ml⁻¹), then transferred to a human MPO₄₃₅₋₄₅₄ coated (10 μ g ml⁻¹) 96-well ELISA plate.

Induction of mouse anti-MPO glomerulonephritis. C57BL/6 mice were immunized subcutaneously at the tail base with either 20 μ g of OVA (control antigen), 20 μ g of rmMPO, 100 μ g of *S. aureus* pSJH101 6PGD₃₉₁₋₄₁₀, 100 μ g of *S. aureus* Variant 3 6PGD₃₉₁₋₄₁₀, 10 mg of heat-killed *S. aureus* JH1, 10 mg of cured heat-killed *S. aureus* JH1, 10 mg of heat-killed *S. aureus* RN4220 transformed with pALC2073 with 6PGD or 10 mg of heat-killed *S. aureus* RN4220 transformed with pALC2073 without 6PGD. Proteins and peptides were injected first emulsified in Freund's Complete Adjuvant (FCA) (day 0), then 7 days later emulsified in Freund's Incomplete Adjuvant (FIA) (day 7). *S. aureus* strains were emulsified in Titermax (Sigma-Aldrich) and injected on days 0 and 7. On day 16, MPO was deposited in glomeruli by recruiting neutrophils using a low dose of intravenously injected heterologous anti-mouse basement membrane antibodies^{9,38,65}. Experiments ended on day 20. Albuminuria was determined by ELISA (Bethyl Laboratories, E90-134) on urine collected 24 h before the end of experiment. Segmental glomerular necrosis was assessed on formalin fixed, paraffin embedded, 3 μ m thick, PAS-stained sections and defined as the accumulation of PAS-positive material with hypocellularity.

CD4⁺ T cells, CD8⁺ T cells, macrophages, and neutrophils were detected by immunoperoxidase staining frozen kidney sections. A minimum of 20 consecutively viewed glomeruli were assessed per animal. The primary mAbs used were clones GK1.5 (anti-mouse CD4; American Type Culture Collection, 20 μ g ml⁻¹), 53-6.7 (anti-CD8a; BioXcell, 10 μ g ml⁻¹), FA/11 (macrophages, anti-mouse CD68; from GL Koch, MRC Laboratory of Molecular Biology, Cambridge, United Kingdom, 10 μ g ml⁻¹), and RB6-8C5 (neutrophils, anti-Gr-1, 2.5 μ g ml⁻¹). MPO-specific delayed type hypersensitivity was measured by intradermal injection of 10 μ g of rmMPO, diluted in PBS, into the left plantar footpad. The same volume of PBS was administered into the contralateral footpad. DTH was quantified 24 h later by measurement of the difference in footpad thickness. IFN- γ , TNF, IL-17A, and IL-6 in rmMPO stimulated splenocyte cultures was measured by cytometric bead array (BD Biosciences, 560485).

Reporting summary. Further information on research design is available in the Nature Research Reporting Summary linked to this article.

Data availability

Source data for Figs. 1, 2, 3b-f, 4, 5b-c, 6-10, and Supplementary Figs. 1-3 are presented in the Source Data file. Other data that support the findings of this study are available from the corresponding author upon reasonable request.

Received: 27 May 2018 Accepted: 26 June 2019

Published online: 29 July 2019

References

- Jennette, J. C. & Nachman, P. H. ANCA glomerulonephritis and vasculitis. *Clin. J. Am. Soc. Nephrol.* **12**, 1680–1691 (2017).
- Xiao, H. et al. Antineutrophil cytoplasmic autoantibodies specific for myeloperoxidase cause glomerulonephritis and vasculitis in mice. *J. Clin. Invest.* **110**, 955–963 (2002).
- Kessenbrock, K. et al. Netting neutrophils in autoimmune small-vessel vasculitis. *Nat. Med.* **15**, 623–625 (2009).
- O'Sullivan, K. M. et al. Renal participation of myeloperoxidase in antineutrophil cytoplasmic antibody (ANCA)-associated glomerulonephritis. *Kidney Int.* **88**, 1030–1046 (2015).
- Huugen, D. et al. Aggravation of anti-myeloperoxidase antibody-induced glomerulonephritis by bacterial lipopolysaccharide: role of tumor necrosis factor- α . *Am. J. Pathol.* **167**, 47–58 (2005).

6. Ooi, J. D. et al. The immunodominant myeloperoxidase T-cell epitope induces local cell-mediated injury in antimyeloperoxidase glomerulonephritis. *Proc. Natl Acad. Sci. USA* **109**, E2615–E2624 (2012).
7. Xiao, H. et al. The role of neutrophils in the induction of glomerulonephritis by anti-myeloperoxidase antibodies. *Am. J. Pathol.* **167**, 39–45 (2005).
8. Chang, J. et al. CD8+ T cells effect glomerular injury in experimental anti-myeloperoxidase GN. *J. Am. Soc. Nephrol.* **28**, 47–55 (2017).
9. Ruth, A. J. et al. Anti-neutrophil cytoplasmic antibodies and effector CD4+ cells play nonredundant roles in anti-myeloperoxidase crescentic glomerulonephritis. *J. Am. Soc. Nephrol.* **17**, 1940–1949 (2006).
10. Hutton, H. L., Holdsworth, S. R. & Kitching, A. R. ANCA-associated vasculitis: pathogenesis, models, and preclinical testing. *Semin. Nephrol.* **37**, 418–435 (2017).
11. Goodnow, C. C. Multistep pathogenesis of autoimmune disease. *Cell* **130**, 25–35 (2007).
12. Lyons, P. A. et al. Genetically distinct subsets within ANCA-associated vasculitis. *N. Engl. J. Med.* **367**, 214–223 (2012).
13. Lamprecht, P. et al. Pathogenetic and clinical aspects of anti-neutrophil cytoplasmic autoantibody-associated vasculitides. *Front. Immunol.* **9**, 680 (2018).
14. Stegeman, C. A. et al. Association of chronic nasal carriage of *Staphylococcus aureus* and higher relapse rates in Wegener granulomatosis. *Ann. Intern. Med.* **120**, 12–17 (1994).
15. Stegeman, C. A., Tervaert, J. W., de Jong, P. E. & Kallenberg, C. G. Trimethoprim-sulfamethoxazole (co-trimoxazole) for the prevention of relapses of Wegener's granulomatosis. Dutch Co-Trimoxazole Wegener Study Group. *N. Engl. J. Med.* **335**, 16–20 (1996).
16. Summers, S. A. et al. Toll-like receptor 2 induces Th17 myeloperoxidase autoimmunity while Toll-like receptor 9 drives Th1 autoimmunity in murine vasculitis. *Arthritis Rheum.* **63**, 1124–1135 (2011).
17. Couser, W. G. & Johnson, R. J. The etiology of glomerulonephritis: roles of infection and autoimmunity. *Kidney Int.* **86**, 905–914 (2014).
18. Salmela, A., Rasmussen, N., Tervaert, J. W. C., Jayne, D. R. W. & Ekstrand, A. Chronic nasal *Staphylococcus aureus* carriage identifies a subset of newly diagnosed granulomatosis with polyangiitis patients with high relapse rate. *Rheumatology* **56**, 965–972 (2017).
19. Glasner, C. et al. Genetic loci of *Staphylococcus aureus* associated with anti-neutrophil cytoplasmic autoantibody (ANCA)-associated vasculitides. *Sci. Rep.* **7**, 12211 (2017).
20. Hellmich, B. et al. Anti-MPO-ANCA-positive microscopic polyangiitis following subacute bacterial endocarditis. *Clin. Rheumatol.* **20**, 441–443 (2001).
21. Miranda-Filloy, J. A. et al. Microscopic polyangiitis following recurrent *Staphylococcus aureus* bacteremia and infectious endocarditis. *Clin. Exp. Rheumatol.* **24**, 705–706 (2006).
22. Kasmani, R. et al. Microscopic polyangiitis triggered by recurrent methicillin-resistant *Staphylococcus aureus* bacteremia. *Int. Urol. Nephrol.* **42**, 821–824 (2009).
23. Tervaert, J. W., Popa, E. R. & Bos, N. A. The role of superantigens in vasculitis. *Curr. Opin. Rheumatol.* **11**, 24–33 (1999).
24. Tadema, H., Heeringa, P. & Kallenberg, C. G. Bacterial infections in Wegener's granulomatosis: mechanisms potentially involved in autoimmune pathogenesis. *Curr. Opin. Rheumatol.* **23**, 366–371 (2011).
25. Birnbaum, M. E. et al. Deconstructing the peptide-MHC specificity of T cell recognition. *Cell* **157**, 1073–1087 (2014).
26. Macdonald, W. A. et al. T cell allorecognition via molecular mimicry. *Immunity* **31**, 897–908 (2009).
27. Harkiolaki, M. et al. T cell-mediated autoimmune disease due to low-affinity crossreactivity to common microbial peptides. *Immunity* **30**, 348–357 (2009).
28. Nelson, R. W. et al. T cell receptor cross-reactivity between similar foreign and self peptides influences naive cell population size and autoimmunity. *Immunity* **42**, 95–107 (2015).
29. Pendergraft, W. F. et al. Autoimmunity is triggered by cPR-3(105–201), a protein complementary to human autoantigen proteinase-3. *Nat. Med.* **10**, 72–79 (2004).
30. Kain, R. et al. Molecular mimicry in pauci-immune focal necrotizing glomerulonephritis. *Nat. Med.* **14**, 1088–1096 (2008).
31. Rossjohn, J. et al. T cell antigen receptor recognition of antigen-presenting molecules. *Annu. Rev. Immunol.* **33**, 169–200 (2015).
32. Mwangi, M. M. et al. Tracking the in vivo evolution of multidrug resistance in *Staphylococcus aureus* by whole-genome sequencing. *Proc. Natl Acad. Sci. USA* **104**, 9451–9456 (2007).
33. Lock, R. J. ACP Broadsheet No 143: January 1994. Detection of autoantibodies to neutrophil cytoplasmic antigens. *J. Clin. Pathol.* **47**, 4–8 (1994).
34. Roth, A. J. et al. Epitope specificity determines pathogenicity and detectability in ANCA-associated vasculitis. *J. Clin. Invest.* **123**, 1773–1783 (2013).
35. Chen, C. J. & Huang, Y. C. New epidemiology of *Staphylococcus aureus* infection in Asia. *Clin. Microbiol. Infect.* **20**, 605–623 (2014).
36. McDougal, L. K. et al. Pulsed-field gel electrophoresis typing of oxacillin-resistant *Staphylococcus aureus* isolates from the United States: establishing a national database. *J. Clin. Microbiol.* **41**, 5113–5120 (2003).
37. Chambers, H. F. & Deleo, F. R. Waves of resistance: *Staphylococcus aureus* in the antibiotic era. *Nat. Rev. Microbiol.* **7**, 629–641 (2009).
38. Gan, P. Y. et al. Th17 cells promote autoimmune anti-myeloperoxidase glomerulonephritis. *J. Am. Soc. Nephrol.* **21**, 925–931 (2010).
39. Nair, D. et al. Whole-genome sequencing of *Staphylococcus aureus* strain RN4220, a key laboratory strain used in virulence research, identifies mutations that affect not only virulence factors but also the fitness of the strain. *J. Bacteriol.* **193**, 2332–2335 (2011).
40. Ooi, J. D. et al. Dominant protection from HLA-linked autoimmunity by antigen-specific regulatory T cells. *Nature* **545**, 243–247 (2017).
41. Grant, E. J. et al. Lack of heterologous cross-reactivity toward HLA-A*02:01 restricted viral epitopes is underpinned by distinct alphabeta T cell receptor signatures. *J. Biol. Chem.* **291**, 24335–24351 (2016).
42. Dendrou, C. A., Petersen, J., Rossjohn, J. & Fugger, L. HLA variation and disease. *Nat. Rev. Immunol.* **18**, 325–339 (2018).
43. Kaplan, M. H. & Meyerserian, M. An immunological cross-reaction between group-A streptococcal cells and human heart tissue. *Lancet* **1**, 706–710 (1962).
44. Kil, K. S., Cunningham, M. W. & Barnett, L. A. Cloning and sequence analysis of a gene encoding a 67-kilodalton myosin-cross-reactive antigen of *Streptococcus pyogenes* reveals its similarity with class II major histocompatibility antigens. *Infect. Immun.* **62**, 2440–2449 (1994).
45. Aires de Sousa, M. et al. Similarity of antibiotic resistance patterns and molecular typing properties of methicillin-resistant *Staphylococcus aureus* isolates widely spread in hospitals in New York City and in a hospital in Tokyo, Japan. *Microb. Drug Resist.* **6**, 253–258 (2000).
46. Wertheim, H. F. et al. Effect of mupirocin treatment on nasal, pharyngeal, and perineal carriage of *Staphylococcus aureus* in healthy adults. *Antimicrob. Agents Chemother.* **49**, 1465–1467 (2005).
47. Acton, D. S., Plat-Sinnige, M. J., van Wamel, W., de Groot, N. & van Belkum, A. Intestinal carriage of *Staphylococcus aureus*: how does its frequency compare with that of nasal carriage and what is its clinical impact? *Eur. J. Clin. Microbiol. Infect. Dis.* **28**, 115–127 (2009).
48. Gagnaire, J. et al. Epidemiology and clinical relevance of *Staphylococcus aureus* intestinal carriage: a systematic review and meta-analysis. *Expert Rev. Anti Infect. Ther.* **15**, 767–785 (2017).
49. Brennan, M. L. et al. Increased atherosclerosis in myeloperoxidase-deficient mice. *J. Clin. Invest.* **107**, 419–430 (2001).
50. Ooi, J. D. et al. The HLA-DRB1*15:01-Restricted Goodpasture's T cell epitope induces GN. *J. Am. Soc. Nephrol.* **24**, 419–431 (2013).
51. Tervaert, J. W. et al. Autoantibodies against myeloid lysosomal enzymes in crescentic glomerulonephritis. *Kidney Int.* **37**, 799–806 (1990).
52. Tervaert, J. W. et al. Occurrence of autoantibodies to human leucocyte elastase in Wegener's granulomatosis and other inflammatory disorders. *Ann. Rheum. Dis.* **52**, 115–120 (1993).
53. Apostolopoulos, J., Ooi, J. D., Odobasic, D., Holdsworth, S. R. & Kitching, A. R. The isolation and purification of biologically active recombinant and native autoantigens for the study of autoimmune disease. *J. Immunol. Meth.* **308**, 167–178 (2006).
54. Broughton, S. E. et al. Biased T cell receptor usage directed against human leukocyte antigen DQ8-restricted gliadin peptides is associated with celiac disease. *Immunity* **37**, 611–621 (2012).
55. Petersen, J. et al. T-cell receptor recognition of HLA-DQ2-gliadin complexes associated with celiac disease. *Nat. Struct. Mol. Biol.* **21**, 480–488 (2014).
56. Peleg, A. Y. et al. Reduced susceptibility to vancomycin influences pathogenicity in *Staphylococcus aureus* infection. *J. Infect. Dis.* **199**, 532–536 (2009).
57. Kuntova, L. et al. Characteristics and distribution of plasmids in a clonally diverse set of methicillin-resistant *Staphylococcus aureus* strains. *Arch. Microbiol.* **194**, 607–614 (2012).
58. Bateman, B. T., Donegan, N. P., Jarry, T. M., Palma, M. & Cheung, A. L. Evaluation of a tetracycline-inducible promoter in *Staphylococcus aureus* in vitro and in vivo and its application in demonstrating the role of sigB in microcolony formation. *Infect. Immun.* **69**, 7851–7857 (2001).
59. Kreiswirth, B. N. et al. The toxic shock syndrome exotoxin structural gene is not detectably transmitted by a prophage. *Nature* **305**, 709–712 (1983).
60. Monk, I. R., Shah, I. M., Xu, M., Tan, M. W. & Foster, T. J. Transforming the untransformable: application of direct transformation to manipulate genetically *Staphylococcus aureus* and *Staphylococcus epidermidis*. *MBio* **3**, e00277–11 (2012).
61. Page, A. J. et al. Comparison of classical multi-locus sequence typing software for next-generation sequencing data. *Microb. Genom.* **3**, e000124 (2017).
62. Feil, E. J., Li, B. C., Aanensen, D. M., Hanage, W. P. & Spratt, B. G. eBURST: inferring patterns of evolutionary descent among clusters of related bacterial genotypes from multilocus sequence typing data. *J. Bacteriol.* **186**, 1518–1530 (2004).

63. Moon, J. J. et al. Naive CD4(+) T cell frequency varies for different epitopes and predicts repertoire diversity and response magnitude. *Immunity* **27**, 203–213 (2007).
64. Moon, J. J. et al. Tracking epitope-specific T cells. *Nat. Protoc.* **4**, 565–581 (2009).
65. Ooi, J. D., Gan, P. Y., Odobasic, D., Holdsworth, S. R. & Kitching, A. R. T cell mediated autoimmune glomerular disease in mice. *Curr. Protoc. Immunol.* **107**, 11–19 (2014). 15–27.

Acknowledgements

This work was funded by an Australian National Health and Medical Research Council (NHMRC) Project Grant (1008849 to A.R.K. and S.R.H.), an NHMRC Center for Research Excellence Grant (1079648 to A.R.K.) and an NHMRC European Union collaborative research grant (1115805 to A.R.K.) as part of the EU Horizon 20/20 RELapses prevention in chronic autoimmune disease (RELENT) Consortium (with P.H.). L.F. acknowledges funding from the Wellcome Trust, the Medical Research Council (UK) and the Oak Foundation. A.Y.P. acknowledges funding from an NHMRC Practitioner Fellowship (1117940). J. Rossjohn is supported by an Australian Research Council Laureate Fellowship.

Author contributions

J.D.O., P.H., A.Y.P., and A.R.K. designed the research and wrote the paper. J.D.O., J.-H.J., P.J.E., L.L.C., M.v.T., K.M.O'S., P.Y.G., and Y.Z. performed and analyzed experiments. K.L.L., H.H.R., and L.F. generated and provided analytical tools. K.T. analyzed data. C.A.S., A.R.K., J. Ryan, and L.R.S. provided samples from healthy humans and people with AAV. S.R.H., L.F., H.H.R. and J. Rossjohn provided intellectual input and technical support.

Additional information

Supplementary Information accompanies this paper at <https://doi.org/10.1038/s41467-019-11255-0>.

Competing interests: The authors declare no competing interests.

Reprints and permission information is available online at <http://npg.nature.com/reprintsandpermissions/>

Peer review information: *Nature Communications* thanks Madeleine Cunningham, J.W. Cohen Tervaert and other anonymous reviewer(s) for their contribution to the peer review of this work. Peer reviewer reports are available.

Publisher's note: Springer Nature remains neutral with regard to jurisdictional claims in published maps and institutional affiliations.



Open Access This article is licensed under a Creative Commons Attribution 4.0 International License, which permits use, sharing, adaptation, distribution and reproduction in any medium or format, as long as you give appropriate credit to the original author(s) and the source, provide a link to the Creative Commons license, and indicate if changes were made. The images or other third party material in this article are included in the article's Creative Commons license, unless indicated otherwise in a credit line to the material. If material is not included in the article's Creative Commons license and your intended use is not permitted by statutory regulation or exceeds the permitted use, you will need to obtain permission directly from the copyright holder. To view a copy of this license, visit <http://creativecommons.org/licenses/by/4.0/>.

© The Author(s) 2019